Estimation of Root Zone Soil Moisture Profile by Reduced-Order Variational Data Assimilation Using Near Surface Soil Moisture Observations

Parisa Heidary, *Member, IEEE*, Leila Farhadi, *Member, IEEE*, and Muhammad Umer Altaf, *Member, IEEE*

***Abstract*—Soil moisture plays an important role in the global water cycle and has an important impact on energy fluxes at the land surface. It also defines the initial and boundary condition of terrestrial hydrological processes, including infiltration, runoff, and evapotranspiration. Therefore, accurate estimation of soil moisture pattern is of critical importance. Satellite-based soil moisture can be obtained with well-defined temporal and spatial resolutions and with global coverage. However, they only provide surface soil moisture at the upper few centimeters of the soil column. Soil moisture simulation models can produce estimates of soil moisture profile up to several meters of depth in different time steps. However, uncertainty in model parameters (e.g., unknown initial soil moisture profile) and meteorological forcing can substantially alter the accuracy of the model estimates. In this article, the potential of using surface soil moisture measurements to retrieve the initial soil moisture profile will be explored in a synthetic study, using two proposed reduced-order variational data assimilation (VDA) techniques and a simple 1-D soil moisture model. The accuracy and feasibility of the proposed approaches are confirmed by comparing the initial soil moisture profiles estimated using the proposed reduced-order VDA techniques versus the full-adjoint VDA technique. Results illustrated that the reduced-order VDA techniques can estimate initial soil moisture profile from near surface soil moisture observations with the comparable level of accuracy as full-adjoint VDA. The effectiveness of the reduced-order VDA in retrieving the initial soil moisture profile is further demonstrated by assimilating surface soil moisture into HYDRUS-1D, mimicking real-world errors.**

***Index Terms*—HYDRUS-1D, proper orthogonal decomposition (POD), Richards equation, soil moisture, variational data assimilation (VDA).**

I. Introduction

SPATIALLY distributed soil moisture profiles are required for land surface and land–atmosphere interaction studies, improving agricultural productivity, assessing drought and flood conditions, estimating groundwater supplies, and landslide prediction. Therefore, measurement and estimation of soil moisture profile and simulation of its pattern play a key role in hydrological research. Soil moisture is extremely variable in space and time because of the dynamics of soil hydraulic properties [1], [2]. Consequently, *in situ* measurement is quite limited for regional and global scale problems [3]. Nonpoint soil moisture measurement techniques exist from local to global scale by using geophysical methods like ground penetrating radar [4], cosmic ray probes [5], ground-based radiometry [6], electromagnetic methods [7], airborne SAR polarimetry [8], airborne L-band radiometry [9], and spaceborne sensors like AQUA/AMSR-E [10], ERS-Scat [11], ASCAT [12], WindSat [13], ENVISAT/ ASAR [14], Advanced Land Observing Satellite (ALOS)/PALSAR [15], Soil Moisture and Ocean Salinity (SMOS)/MIRAS [16], and SMAP [17], [18]. The benefits of spaceborne platforms, which use active (ALOS) or passive (SMOS) microwave sensors, are global coverages and well-defined temporal resolutions [2]. However, remote microwave sensors provide only the spatial pattern of soil moisture for the upper few centimeters of a soil column and direct sensing of the spatiotemporal distribution of root zone soil moisture still remains a challenge.

Soil moisture simulation models, generally called soil vegetation atmosphere transfer (SVAT) models, can produce estimates of soil moisture profile to several meters of depth on different (e.g., hourly, daily, and monthly) time steps. The accuracy of the model simulated soil moisture profile depends on the model physics, the number and configuration of soil layers, and the accuracy and nature of input data and the initial conditions (i.e., initial soil moisture profile) [19]. Initial soil moisture profile is a crucial factor that influences the water storage capacity of the soil column as well as the soil hydraulic properties [20]. Therefore, initial soil moisture profile plays a key role in infiltration, and hence the time evolution of the profile of soil moisture (e.g., [21], [22]). The significant impact of initial soil moisture profile on the infiltration rate was investigated in a variety of studies over the past few decades (e.g., [20], [22]–[27]). Numerous modeling studies have shown the high sensitivity of the modeled hydrological responses such as runoff to initial soil moisture profile used in the hydrological models (e.g., [23], [28], [37], [38], [29]–[36]) and in the ability of land surface models to predict extreme events such as floods and droughts (e.g., [39]–[41]). Therefore, overcoming the challenge of inputting an accurate initial soil moisture profile to SVAT models can significantly impact the accuracy of the temporal evolution of soil moisture profile, hence prediction of hydrological responses.

Manuscript received September 21, 2021; revised January 3, 2022; accepted January 20, 2022. Date of publication February 4, 2022; date of current version March 25, 2022. This work was supported in part by the NSF CAREER Award #1944457 (PI: L. Farhadi, GWU) and in part by the US Geological Survey Award #2020DC119B (PI: L. Farhadi, GWU). *(Corresponding author: Leila Farhadi.)*

Parisa Heidary and Leila Farhadi are with the Department of Civil and Environmental Engineering, George Washington University, Washington, DC 20052 USA (e-mail: parisaheidary@gwu.edu; lfarhadi@gwu.edu).

Muhammad Umer Altaf is with the King Abdullah University of Science and Technology, Thuwal 23955, Saudi Arabia (e-mail: umer.altaf@kaust.edu.sa).

Digital Object Identifier 10.1109/JSTARS.2022.3147166

Combining the horizontal coverage and spatial resolution of remote sensing with the vertical coverage and temporal continuity of a soil moisture simulation model provides an opportunity to estimate the temporal evolution of soil moisture profile with minimum uncertainty (e.g., [42], [43]). A considerable amount of literature has been conducted on exploring the ability to use satellite surface soil moisture to estimate the profile of root zone soil moisture. Kostov and Jackson [44] provided a comprehensive review of the methods of estimating soil moisture profile using remote sensing techniques. They concluded that the assimilation of remote sensing surface soil moisture into the physical model through inverse modeling and data assimilation techniques is the most promising method to improve the estimation of the profile of soil moisture. A detailed review of the state- of-the art data assimilation techniques used for the estimation of the soil moisture is provided in [45]. There are two distinct classes of data assimilation methods, both capable to account for imperfect parameters (e.g., unknown initial conditions). One is the variational techniques, which search for an optimal set of control variables/parameters, such that a cost function that measures the distance between the model and observations is minimized. The second class assimilates observations in a sequential manner referred to as sequential methods, namely Kalman filtering. In sequential approaches, the state of the system with highest probability is identified based on the assumption of linear dynamical model and Gaussian distribution of error terms and the estimated variables are corrected every time an observation becomes available [46], [47]. While numerous studies have successfully applied Kalman filtering to assimilate surface soil moisture into a land surface model to improve predicted model state variables (e.g., soil moisture and soil temperature) (e.g., [48]–[57]), when it comes to estimation of parameters (e.g., unknown initial soil moisture profile), Kalman filtering methods can lead to unstable results due to a complex interactions between states and parameters [58]–[61]. The Kalman filter conducts parameter estimation by augmenting the state vector with the uncertain parameters [62]. Generally, this approach performs well in case of noisy parameters that slowly vary in time and, therefore, act like states [63]. This filter is biased for constant parameters that are not affected by noise [64] and tends to diverge from the optimal results when parameters are constant (e.g., the case of unknown initial soil moisture profile) [62].

Variational data assimilation (VDA), also known as the "adjoint" method, is one of the most powerful and robust approaches for parameter estimation/model calibration (e.g., [65]–[67]). This method aims at calibrating a number of unknown parameters based on given data, where the unknown parameters can be the model initial conditions or any other model parameters and inputs. This method is well-suited for the highly nonlinear soil moisture estimation problems, where usually optimal estimates of either the physical model parameters or model initial condition (e.g., unknown root zone soil moisture profile) are obtained through assimilation of surface state observations (i.e., surface soil moisture) or surface brightness temperature into an SVAT model [68]. The VDA/adjoint method estimates the unknown parameters by defining a cost function, which measures the misfit between the observation and model estimate of the observation over the assimilation interval/window. The cost function will then be minimized with respect to the unknown parameters using gradient-based optimization techniques to achieve the optimal solution. The calculation of the gradient of the cost function in VDA/adjoint method is very efficient as it is independent of the number of unknown parameters and requires only a single simulation of the model forward in time and a single simulation of adjoint model backward in time (e.g., [47], [69]–[73]). However, the integration of the adjoint of a large-scale model backward in time may require several forward model simulations that increase the computational burden and expense of this technique [74]–[76]. Another drawback of the VDA/adjoint method is the importance of human and computing resources that are required for the implementation, maintenance, and the execution of the adjoint of highly nonlinear systems (e.g., SVAT models). Automatic differentiation tools generate the adjoint of a computer code through direct compilation, and adjoint compilers are available [75], [77]. However, even with the presence and use of these adjoint compilers, developing the adjoint model still requires significant programming efforts that hinders new applications of the VDA/adjoint method for parameter estimation. Moreover, any modification to the forward model necessities the modification of the adjoint, hence, making it imperative to keep track of the model code development [78]. Early attempts to overcome the difficulties related to the computation of adjoint have focused on the simplification and approximation of the adjoint model [70]. One way to overcome this complexity is reducing the space size of the parameters. This can be achieved by replacing the original model by a fast lower resolution model that approximates the original model (e.g., [79]) or simplifying the model physics before building the adjoint (e.g., [80]). Hence, they can be practical in large-scale highly nonlinear hydrological/land surface models used in numerical weather prediction, global climate, and earth system modeling. Reduced-order techniques can also be used to apply the VDA problem on efficient low-order approximate linear models for which the adjoint code can be easily developed (e.g., [81]).

Proper orthogonal decomposition (POD), as a model reduction technique, is the application of the singular value decomposition to the approximation of general dynamical systems. By processing the data obtained from numerical simulations of the model, which is expected to summarize information about the dynamical behavior of the system, POD method defines the reduced or projected subspace [78], [82]. Vermeulen and Heemink [63] proposed a POD-based numerically efficient model-reduced VDA method (hereafter, MR-VDA), where a reduced-order model that is linear and easy to integrate, is built numerically using finite differences applied in the POD-reduced space. The reduced adjoint is then obtained easily and the optimization is completely conducted in the POD space with a very low computational cost [83]–[85]. A drawback of this method is that optimization (i.e., minimization of model-data misfit terms) is fully applied in the reduced POD space and this could lead to an optimized set of parameters that is not a solution of the original variational problem [78]. To address this potential

drawback, Altaf *et al.* [78] proposed a simple modification to the MR-VDA approach of Vermeulen and Heemink [63]. The idea was to solve exactly the original VDA problem where the model-data misfit terms in the cost function are computed in the original full space, but using approximate gradients that are computed as the outputs of the POD-reduced-adjoint model. The proposed reduced-adjoint VDA (hereafter, RA-VDA) not only avoids the implementation of the adjoint of the original nonlinear model, but is also shown to be very efficient, in terms of computation cost and performances [47], [78], [86]. The goal of this article is 1) to explore the potential of reduced-order VDA techniques (MR-VDA and RA-VDA) as a replacement for full-adjoint VDA which requires lots of differentiation that can make this technique impractical for large-scale highly nonlinear hydrological/land surface models and 2) to show the effectiveness of these reduced-order approaches in estimating the initial condition for such highly nonlinear models in order to produce temporal estimates of soil moisture profile with reduced uncertainty.

The specific objectives of this article are: 1) analyzing the feasibility of the VDA approaches (reduced-order and full-order) to retrieve the initial soil moisture profile by assimilating surface soil moisture into a simple, easily differentiable soil moisture simulation model; 2) examining the potential of using reduced-order VDA as a comparative alternative to full-adjoint VDA for soil moisture estimation; 3) illustrating the effectiveness of the proposed reduced-order VDA techniques in retrieving the initial soil moisture profile by assimilating surface soil moisture observations into a highly nonlinear SVAT model; and 4) investigating the performance of the reduced-order VDA approaches in estimation of the soil moisture profile, in presence of error by mimicking real-world observational and forcing errors. To this end, in this article, we present three synthetic (twin) experiments using proposed VDA approaches and forward models (i.e., Richards model and HYDRUS-1D model) simulating soil water dynamics. Synthetic experiments make it possible to understand the model response to state updates and draw the effects of model and observation uncertainties. Such experiments are irreplaceable tools for assessing the performance of the assimilation algorithm. They provide a benchmark for interpreting the results of different case studies and a basis to direct the development of land data assimilation systems and remote sensing algorithms in order to improve the predictions [45], [87]. Hence, our findings will help to assess the value of spaceborne observations of surface soil moisture for initial soil moisture profile estimation.

The rest of this article is organized as follows. Section II-A depicts the physical soil moisture simulation models used in this article. Section II-B introduces the VDA framework for the estimation of the unknown parameters. Sections II-C and II-D describes the construction of the POD-reduced space and the POD-based model reduction procedure for minimization, respectively. Section III explains the experiments and dataset by which the VDA approaches (full-adjoint VDA, RA-VDA, and MR-VDA) are tested. In Sections IV and V, the results and conclusion are presented, respectively.

II. Methodology

A. Forward Models

Following [63], a dynamical system is modeled by a discrete nonlinear equation of the form:

$$\theta\left(t_{i+1}\right) = F_i\theta\left(t_i\right),\ i = 1, 2, \ldots, m-1 \tag{1}$$

where $\theta(t_{i+1}) \in R^n$ is a model state vector, $F_i : R^n \rightarrow R^n$is a nonlinear dynamics operator, known as the forward model that propagates the state from t_i to time t_{i+1}. The forward models used in this article are Richards Model (Section II-A-1) used in experiment 1 and HYDRUS-1D model (Section II-A-2) used in experiments 2 and 3.

1) 1-D Richards Model: The simple, easily differentiable 1-D Richards model is developed based on the well-known Richards equation [88], [89], where the movement of water/flow in the unsaturated column of soil is simulated by a combination of Darcy's law and the mass conservation equation, yielding the 1-D Richards equation:

$$\frac{\partial\theta}{\partial t} = \frac{\partial}{\partial z}\left(K\frac{\partial h}{\partial z} - K\right) - S(z,t). \tag{2}$$

In (2), Θ is the volumetric water content (cm^3cm^{-3}), t is the time (h), z is the vertical dimension and is positive downward (cm), h is the pressure head (cm), which becomes negative for unsaturated conditions. $K(h)$ is the unsaturated hydraulic conductivity function. S is the sink term, water uptake from plant roots, related to the transpiration (T) from canopies. Typically, $S(z, t)$ depends on many factors such as the density of roots in the root zone, soil water content, and atmospheric demand [89]. In this article, transpiration from the canopy and consequently $S(z, t)$ are neglected.

Soil moisture profile estimation at different depths via Richards model depends on the boundary fluxes entering and leaving the soil column and initial soil moisture profile as the initial condition. In this article, the common gravitational drainage is used as the bottom boundary condition by setting $q_{Z=Z_b} = K$ [72], [90]. The surface boundary condition may change from a head-controlled to a flux-controlled and vice versa [91], [92]. At moderate weather, flux controls the surface boundary condition (flux-controlled boundary condition) and the net flux (q) results from precipitation (P), evaporation (E), and runoff (R_{OFF}) as (3). In this article, it is assumed that the precipitation rate (cm/h) is less than the saturated hydraulic conductivity, and land stores water in its depression storage and preventing it from flowing, so the surface runoff is neglected:

$$q_{z=0} = P - E - R_{off}. \tag{3}$$

At too-wet weather, a head-controlled boundary condition handles the surface boundary condition in such a way that the infiltration flux is controlled by the head of water at the soil surface. At too-dry weather or dry soil conditions, the head of water at the soil surface adapts to the air humidity and controls the evaporation flux [72], [93].

The hydraulic properties of unsaturated soil here are parameterized using the widely used Brooks and Corey model [94]

$$h = h_{sat}\left(\frac{\theta}{\theta_{sat}}\right)^{-B} \tag{4}$$

$$K = K_{sat}\left(\frac{\theta}{\theta_{sat}}\right)^{2B+3} \tag{5}$$

where $h_{\rm sat}$, $K_{\rm sat}$, and $\Theta_{\rm sat}$ are saturated soil matric potential, hydraulic conductivity, and soil water content, respectively; these parameters are the functions of the soil texture. *B* is a function of pore size index. In this article, the value of $\theta_{\rm sat}$, $K_{\rm sat}$, $h_{\rm sat}$, and *B* are approximated based on the soil texture from the look-up table [95].

In the 1-D Richards model, for a given initial soil moisture profile, the Richards equation is solved using finite differences (forward in space and fully implicit in time) employing a simple linearization scheme to determine the temporal derivative of the soil moisture profile.

2) The HYDRUS-1D Model: HYDRUS-1D is a software package developed by [96] to simulate water, heat, and solute movement in 1-D variably saturated porous media. It is a physically based model that numerically solves the 1-D Richards equation using Galerkin-type linear finite-element schemes. In experiments 2 and 3 of this article, HYDRUS-1D is used as the forward model. For the parametrization of hydraulic conductivity and soil water retention function, the Mualem van Genuchten parameterization [97] is used. The same boundary conditions, as explained in Richards model section, are applied here.

B. Full-Adjoint Variational Data Assimilation (Full-Adjoint VDA)

The imperfect observation $Y(t_i) \in R^q$ of a dynamical system [shown in (1)] that is related to the model state at time t_i through the observation operator $H_i : R^n \to R^q$ is defined as

$$Y(t_i) = H(\theta(t_i)) + \eta(t_i). \tag{6}$$

Operator *H* maps the model fields on observation space, $\eta(t_i)$ accounts for the imperfection in the observations (e.g., measurement errors), and is assumed to be a white Gaussian observation noise process with zero mean and covariance matrix R_i. The objective of VDA is to find an optimal set of parameters that provides the best model fit with available observations, measured through an objective cost function. Since the focus of this article is to estimate the initial soil moisture profile, θ_0 (a vector of soil moisture at different depth of soil) is considered as the control parameter. The objective function *J* to be minimized is defined as

$$J(\theta_0) = \frac{1}{2}\left(\theta_0 - \theta^b\right)^T B_0^{-1}\left(\theta_0 - \theta^b\right) + +\frac{1}{2}\sum_{i=0}^{m}\left(Y(t_i) - H(\theta(t_i))\right)^T R_i^{-1}\left(Y(t_i) - H(\theta(t_i))\right) \tag{7}$$

where θ^b is a prior estimate of θ_0, assumed uncorrelated with covariance matrix B_0. The second term is the misfit between real observations and model estimated observations. The errors in the observations and the errors in the prior estimates are assumed to be uncorrelated. The cost function will be minimized over the window of available data and constrained by the model dynamics [i.e., the forward model (2)]. The minimization of *J* is often based on gradient-based methods and requires the computation of ∇J with respect to θ_0. The most efficient method to compute the gradient of the cost function is the adjoint method [78], [98], [99]. In this method, the gradient of the cost function is computed by chain rule for differentiation [78]. To formulate the adjoint method, Lagrange multiplier method is used to transform the constrained optimization problem to an unconstrained optimization problem. Hence, the physical constraint (i.e., the forward model propagating the state in time) is adjoined to the cost function *J*. In this method, the Lagrange multiplier is denoted by $\upsilon(t_i)$ and is often referred to as the adjoint state variable (i.e., the state variable of the adjoint equation). The optimum values of the parameters are obtained by setting the ∇J equal to zero. This leads to the adjoint equation, which is solved backward in time from t_m to t_0 to calculate the adjoint state variable/Lagrange multipliers υ at each time (see [78] for details).

C. Proper Orthogonal Decomposition (POD)

POD, also known as principal components analysis in statistics, is used for a broad range of model-reduction applications (see [82]). In general, model-reduction methods aim to produce a low-dimensional system that has the same response characteristics as the original system [63], [78], [82]. The main idea of POD is to find a subspace W_r within a vector space *W*, in such a way that the error in the projection onto the subspace is minimized. This method uses an orthogonal transformation to convert a set of possibly correlated variables into a set of linearly uncorrelated variables called POD modes. POD modes describe the dominant behavior or dynamics of the given problem [86].

A set of snapshots of a physical model are collected from an experiment or a numerical simulation of a dynamical system to create the POD modes. The snapshot should be able to describe the model's response to the unknown parameters. Each sample of snapshots θ_i stands for an *n*-dimensional vector θ_{jn} that is $\theta_i = \{\theta_{i1}, \theta_{i2}, \ldots, \theta_{in}\}\ i \in \{1, 2, \ldots, s\},\ s < n$, where *s* is the number of snapshots and *n* is the total number of the ensemble. Then, a "centered" ensemble *E* is formed by means of the mean vector $\bar{\theta}$

$$E_i = \theta_i - \bar{\theta}. \tag{8}$$

To create POD modes, first, the covariance matrix of *E* needs to be found, which can be calculated by

$$Q = \frac{1}{s-1}EE^T. \tag{9}$$

The algorithm here contains a large eigenvalue problem for a full matrix $Q \in R^{n\times n}$, which is computationally expensive. To overcome this issue, the method of snapshots (proposed by [100]) is used and instead of solving the eigenvalue problem

for the matrix $Q \in R^{n\times n}$, one only needs to find the eigenvalues of $Q' \in R^{s\times s}$ [101] which is defined as $Q' = \frac{1}{s-1}E^T E$. Eigenvectors of the covariance matrix are orthogonal that are used to reorient the data from x and y axes to the axes represented by PODs. Using eigenvalues and eigenvectors of the covariance matrix, the POD modes p_i are computed by

$$p_i = EZ_i/\sqrt{\lambda_i} \tag{10}$$

where Z_i are eigenvectors and λ_i are eigenvalues of Q'. Z points into the direction of the largest spread of the data, and whose magnitude equals the spread in this direction. The largest eigenvector of the covariance matrix always points into the direction of the largest variance of the data; the magnitude of this vector equals to the corresponding eigenvalue. Then, the eigenvalues are used to find a measure of the relative variance (11) of the corresponding POD modes:

$$\varphi_i = \frac{\lambda_i}{\sum_{l=1}^{s}\lambda_l}.100\%\,, \quad i = \{1,\, 2,\, \ldots,\, s\}\,. \tag{11}$$

Note that $r < s << n$ and $\varphi_1 > \varphi_2 > \ldots > \varphi_{\mathrm{r}}$. Please note that the number of POD modes that are retained (i.e., r) should be small enough to assure a fast convergence rate at the beginning of the optimization and large enough (up to a certain level because the last POD modes usually show noise) to efficiently display the variability of the original full space [102].

D. Reduced-Order VDA

1) Model-Reduced VDA (MR-VDA): The main idea of using model order reduction to approximate the adjoint equation is to replace the original full space model by its POD-derived approximate. The approximate state here is

$$\hat{\theta}\,(t_i) = P\xi\,(t_i) + \theta^b \tag{12}$$

where θ^b, as introduced in B is the background state, often taken as a mean state, the matrix P contains the dominant POD modes of the system dynamics operator F_i and satisfies P^T. The approximate state $\hat{\theta}(t_i)$ is a linear combination of the dominant POD modes, and $\xi(t_i)$, the reduced state vector, which contains the corresponding coefficients. It evolves in time according to

$$\xi\,(t_{i+1}) = \tilde{F}_i\xi\,(t_i) \tag{13}$$

where the reduced dynamical operator $\tilde{F}_i$ can be computed as

$$\tilde{F}_i = P^T\left(\frac{\delta F_i}{\delta\theta\,(t_i)}p_1,\, \ldots,\, \frac{\delta F_i}{\delta\theta\,(t_i)}p_r\right). \tag{14}$$

To compute the components of $\tilde{F}_i$, finite difference approach is used to linearize the original forward model F (1) with respect to $\theta(t_i)$ along the direction of the dominant POD modes p_i [63]:

$$\frac{\delta F_i}{\delta\theta\,(t_i)}p_h = \frac{F_i\left[\theta\,(t_i) + \varepsilon p_h\right] - F_i\left[\theta\,(t_i)\right]}{\varepsilon}. \tag{15}$$

ε is the size of the perturbation. In the model reduced approach, we look for an optimal solution of (1) that minimizes the approximate cost function $\hat{J}$:

$$\begin{aligned}\hat{J}\ (\xi_0) = {} & \frac{1}{2}\left(P^T\left(\theta^b - \theta_0\right)\right)^T P^T B_0^{-1} P\left(P^T\left(\theta^b - \theta_0\right)\right) \\ & + \frac{1}{2}\sum_i\left(Y\,(t_i) - H\left(\hat{\theta}\,(t_i)\right)\right)^T R_i^{-1}\left(Y\,(t_i)\right. \\ & \left. -H\left(\hat{\theta}\,(t_i)\right)\right).\end{aligned} \tag{16}$$

Since the reduced model is linear, its adjoint in the reduced space is easy to obtain and the backward evolution equation for the adjoint state variable $\hat{\nu}(t_i)$ is defined as

$$\hat{\nu}\,(t_i) = \tilde{F}_i^T\hat{\nu}\,(t_{i+1}) + P^T H^T R_i^{-1}\left(Y\,(t_i) - H\hat{\theta}\,(t_i)\right). \tag{17}$$

Then, the gradient of the approximate cost function is calculated in reduced space size by

$$\nabla\hat{J}\,(\xi_0) = -P^T B_0^{-1} P\xi_0 - \hat{\nu}\,(t_0)\,. \tag{18}$$

In this approach, the optimization is performed in the POD-reduced space by setting $\nabla\hat{J}$ equal to zero [63], [69]. While this type of simplification accelerates the convergence, there is no guarantee that the minimum found with this approach is also the global minimum in the full space [47], [78].

2) Reduced-Adjoint VDA (RA-VDA): A new reduced-adjoint approach is proposed by [78] where the forward model remains the same as (1). This means that we look for an optimal solution of (1) to minimize the same cost function J (7) in the original space size, while the adjoint model is built in reduced space by projecting the adjoint states on the dominant POD modes. The equation for adjoint state is then expressed as follows:

$$\hat{\nu}\,(t_i) = \tilde{F}_i^T\hat{\nu}\,(t_{i+1}) + P^T H^T R_i^{-1}\left(Y\,(t_i) - H\theta\,(t_i)\right). \tag{19}$$

This equation is solved backward in time, given $\hat{\nu}\,(t_m) = 0$. The gradient of the cost function is then calculated in original space size given by

$$\nabla J\,(\theta_0) = -B_0^{-1}(\theta_0 - \theta^b) - P\hat{\nu}\,(t_0)\,. \tag{20}$$

Once the gradient (∇J) is obtained, the minimization of the cost function is conducted along the direction of gradient in the original space. Note the difference between the adjoint model in MR-VDA and RA-VDA is shown in (17) and (19), respectively. As indicated in these equations, to obtain the reduced adjoint state in the RA-VDA, the system state (θ) is constrained by observations Y, while in MR-VDA, the reduced system state ($\hat{\theta}$) is constrained by observations. This means that in RA-VDA approach, in order to compute the adjoint state, the original forward model (1) needs to be integrated for every optimization iteration while, for the MR-VDA approach, the POD-reduced model (12) needs to be integrated for every optimization iteration. The flowcharts of the initial soil moisture profile estimation with full-adjoint VDA, RA-VDA, and MR-VDA are provided in Fig. S1.

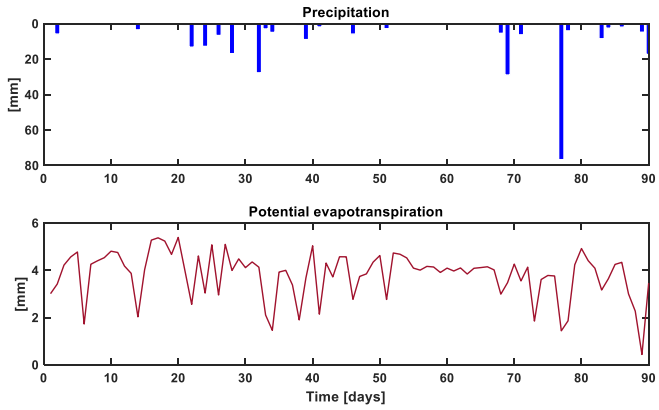

Fig. 1. Daily precipitation and potential evaporation time series at the FIFE experimental site (28 May 1987 to 25 August 1987).

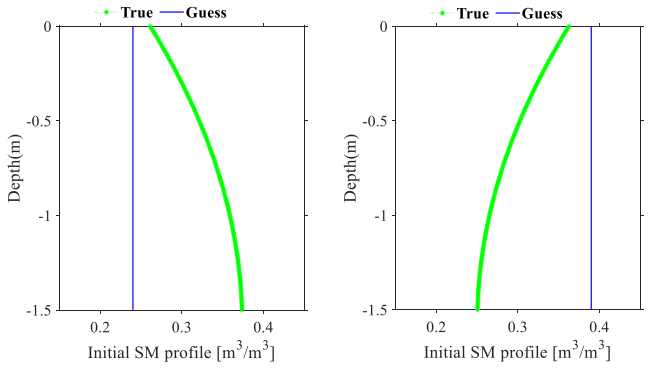

Fig. 2. Synthetic true setup, (right) dry case, (left) wet case—blue: i itial guess for the initial soil moisture profile, green: the synthetic true initial soil moisture profile. SM: Soil Moisture.

TABLE I
ASSUMED HYDRAULIC PARAMETERS BASED ON THE LOOK-UP TABLE PROPOSED BY [105]

Parameter		Description
K_S (m/day)	0.2376	Saturated hydraulic conductivity
θ_S (m^3/m^3)	0.47	Saturated soil moisture
h_S (m)	-0.44	Saturated soil matric potential
B (-)	5.68	Soil parameter that describes the shape of the water release characteristic
WP (m^3/m^3)	0.168	Wilting point

III. DATASET AND EXPERIMENT SETUP

In this article, the forcing and meteorological data (i.e., precipitation, maximum/minimum air temperature, wind speed, relative humidity, and net radiation) were taken from the FIFE experiment near Manhattan, Kansas [103]. The simulation period is 90 days from May 28 to August 25 on a daily basis. The potential evapotranspiration was calculated with the Penman–Monteith combination equation provided by FAO [104]. The daily time series of precipitation and potential evapotranspiration of the study area are shown in Fig. 1. The average precipitation and potential evapotranspiration over 90 days are 3.2 and 3.8 mm, respectively. As can be seen, the precipitation is not distributed evenly.

The soil type falls in the texture classes of silty clay loam (33.33% clay, 13.33% sand, and Bulk density is 1.34). The effective hydraulic parameters used in Richards model, shown in Table I, are obtained using the look-up table proposed by [105]. The parametrization of hydraulic conductivity and soil water retention function in HYDRUS-1D model is obtained by neural network prediction in the software using soil texture information. The other assumption that is used in this article is that there is no vegetation cover, so LAI value is zero in both Richards model and HYDRUS-1D. The flow domain of the soil profile is 150 cm with a spatial discretization of 1 cm in the Richards model and variable discretization of 1 cm for the first 50 cm, 2 cm for the second 50 cm, and 3 cm for the last 50 cm depth is used in the HYDRUS-1D model.

Different numerical experiments are designed to address the objectives of this article. Experiment (1) is designed to test the feasibility of the VDA approaches (full-adjoint and reduced-order VDA) and evaluate their accuracy in estimating the initial soil moisture profile from surface soil moisture observations. To focus on the efficiency and accuracy of the variational approaches in retrieving initial soil moisture profile, the assimilation is operated under ideal condition and the observations in these experiments are the synthetic true surface soil moisture. The ideal condition here means that the same physical model, the same meteorological forcing and inputs, and the same error statistics are used for generating both the synthetic truth and the assimilation. Ideal condition experiments are used to test the assimilation algorithm, detect coding errors, and evaluate the effects of nonlinearities on the estimation. Consequently, observing system characteristics can be evaluated and optimized through ideal experiments. To develop the full-adjoint VDA algorithm a simple, easily differentiable 1-D Richards model (see Section II-A-1) is used. Thus, the synthetic datasets (hereafter, true) for experiment 1, are produced by running the Richards model for two distinct initial soil moisture profiles as the initial condition (Fig. 2). The first case represents a dry surface condition where the initial soil moisture profile increases with depth starting from 0.25 (m^3/m^3) at the surface (top node) to 0.38 (m^3/m^3) at the bottom node of the soil profile. These values are selected to be between the wilting point and the saturation point. The second case represents wet surface soil moisture condition and the soil moisture decreases with depth from 0.38 (m^3/m^3) at the top node to 0.25 (m^3/m^3) at the bottom node. Having the true initial soil moisture profile, the synthetic soil moisture is generated from the forward model run. Average of top 5 cm of the soil moisture is considered as the surface soil moisture observations. Then the assimilation process starts by assimilating the surface soil moisture observations into the same physical model (i.e., Richards model), under ideal conditions via the proposed VDA approaches (i.e., full-adjoint VDA, RA-VDA, and MR-VDA) to retrieve the initial soil moisture profile.

Experiment (2) is designed to test and illustrate the efficiency and accuracy of the proposed reduced-order VDA techniques (RA-VDA and MR-VDA) in estimating initial soil moisture profile by assimilating surface soil moisture observations into a highly nonlinear SVAT model. In this experiment, the HYDRUS-1D model [106] (a well-known SVAT model for predicting soil moisture content and water movement in soil) is used as a forward model to generate synthetic true soil moisture profile. Similar to experiment (1), the assimilation algorithm

TABLE II
FORCING DATA PERTURBATION VALUES

Forcing Data	Perturbation Model	Mean	Standard Deviation	Unit
Precipitation	Multiplicative lognormally distributed	1	0.5	cm/day
Net Radiation	Multiplicative lognormally distributed	1	3	MJ/m^2d
Temperature (Max and Min)	Additive Gaussian	0	3	°C
Humidity	Additive Gaussian	0	5	%
Wind Speed	Additive Gaussian	0	250	km/day

here is operated under ideal conditions and the accuracy of MRA-VDA and RA-VDA in retrieving initial soil moisture profile is evaluated.

Experiment (3) is designed to further investigate the performance of the proposed reduced-order VDA methods in estimation of the initial soil moisture profile using HYDRUS-1D, under nonideal conditions. To this end, two scenarios are implemented to determine the performance of the assimilation algorithm in presence of 1) observation uncertainty, and 2) modeling and observation uncertainty. The observation uncertainty is considered by adding randomly generated Gaussian noise with zero mean and maximum 0.03–0.04 variance to the surface soil moisture time series obtained from the synthetic truth. The model uncertainty is prescribed to weather inputs by perturbing daily forcing variable following [87] as shown in Table II.

IV. RESULTS AND DISCUSSION

A. Experiment 1

Including figures and tables, the performance of the proposed VDA methods (i.e., full-adjoint VDA, RA-VDA, and MR-VDA) in estimating the true initial soil moisture profile is explored through assimilation of surface soil moisture observation into the Richards model through a synthetic study (explained in Section III). Given that in a synthetic study, the true system is exactly known and it is used for model performance tests.

Perfect observations (truth) were generated from the simulated reference surface soil moisture time series via Richards model using the synthetic true initial soil moisture profile. According to [107], the synthetic true initial soil moisture profile is assumed to have a second-order polynomial form as a function of subsurface depth. As such, two cases are selected as the true initial soil moisture profile, shown in Fig. 2 (explained in Section III), dry case: increasing moisture with depth and wet case: decreasing moisture with depth.

The goal of the VDA approaches is to find the optimal values of unknown parameters (e.g., initial soil moisture profile) by minimizing the cost function described in Subsection B. To start the minimization process, the initial guess for the initial soil moisture profile (θ_0) from which the forward model simulation starts is chosen as uniformly distributed in depth, with a magnitude that is within the margin of error of surface soil moisture observation (obtainable through remote sensing) (as shown in Fig. 2).

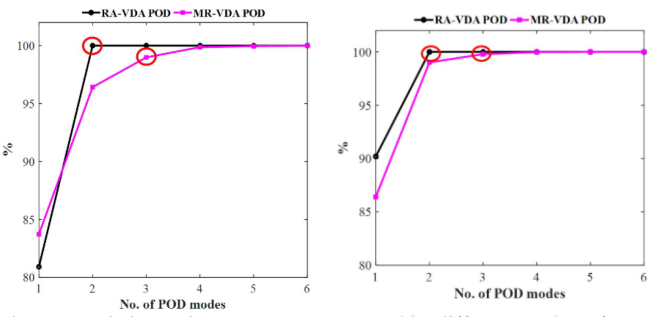

Fig. 3. Cumulative variance percentage covered by different number of POD modes, (right) dry case, and (left) wet case.

To compute the POD basis vectors for the reduced-order VDA approaches, the forward model is run with the initial guess. Then, an ensemble E of 90 snapshots vectors are created. The snapshots are collected over a regularly spaced interval of every day. Using this ensemble E, the matrix P that consists of dominant POD modes and captures over 98% of the variance of the data is created. Fig. 3 shows the increase in cumulative variance retained versus the number of POD modes for both dry and wet cases. As seen in this figure, in MR-VDA and RA-VDA, three POD modes and two POD modes represent the variability of the dataset (i.e., captures over 98% of variance of the data), respectively.

In the reduced-order VDA approaches, the estimations are highly dependent on the size of the perturbation (defined in (15)] for constructing the reduced dynamical model. The stopping criteria (convergence criteria) for the optimization is defined as

$$\mu = \frac{|J_{m+1} - J_m|}{\max\{J_{m+1}, 1\}} < \sigma. \tag{21}$$

The value of σ is chosen such that the difference in cost function J in two successive iterations is minuscule, e.g., $\sigma = 1e{-}6$. For the optimization algorithm, a quasi-Newton method with BFGS (Broyden–Fletcher–Goldfarb–Shanno) [108] updating algorithm for the hessian is used. Fig. 4 shows the reduction in the value of the cost function for both wet and dry cases, until a plateau is reached and changes between two iterations become negligible. As it is shown in Fig. 4, for both dry and wet cases, the full-adjoint VDA method achieves the largest decrease in the value of cost function, albeit with a lower convergence rate (higher number of iterations) and less complexity associated with the derivations of the adjoint. In terms of convergence rate, MR-VDA is the fastest. In MR-VDA (RA-VDA), the cost function drops down and converges to the optimum solution by reaching the plateau after 8 (183) iterations for dry case and after 11 (152) iterations for wet case, while for the full-adjoint VDA the numbers are 333 iterations and 350 iterations, respectively (see Table III). As seen in the table, both RA-VDA and full-adjoint have a comparable reduction of over 90% reduction in cost function for both dry and wet case, while in MR-VDA the cost function is reduced 82.56% for dry case and 95.88% for the wet case.

The performance of the three variational approaches in the estimation of the initial soil moisture profile for both dry case

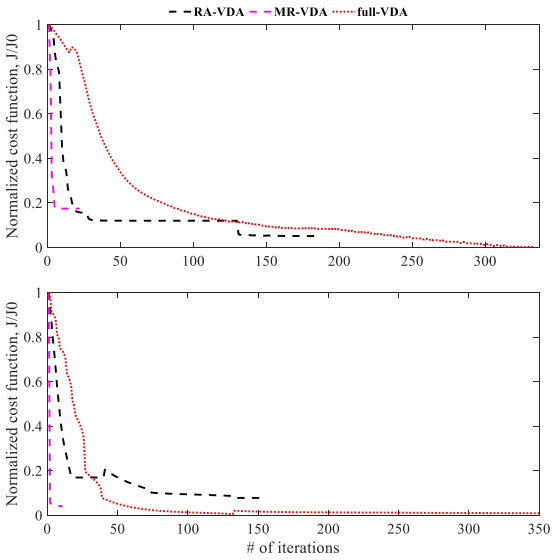

Fig. 4. Successive minimization iteration of the cost function J with (a) RA-VDA method (black), (b) full-adjoint VDA method (red), and (c) MR-VDA (magenta) for dry case (top) and wet case (bottom).

TABLE III
PERCENT REDUCTION (ITERATION NUMBER) IN THE VALUE OF THE NORMALIZED COST FUNCTION $\Delta J/J0$ FOR DRY CASE AND WET CASE

	ΔJ/J0 (# iteration)		
Method	Full-adjoint VDA	RA-VDA	MR-VDA
Dry case	99.74% (333)	94.92% (183)	82.56% (8)
Wet case	99.44% (350)	92.21% (152)	95.88 (11)

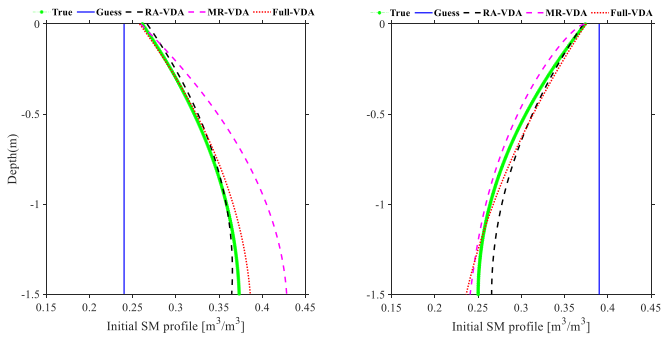

Fig. 5. Estimated initial soil moisture profile with RA-VDA method (black), MR-VDA method (magenta), and full-adjoint VDA method (red) comparing with the true (green) and initial guess (blue). (a) Dry case (left). (b) Wet case (right).

and wet case is illustrated in Fig 5. As seen in this figure, the final estimation of the initial soil moisture profile in both reduced-order VDA approaches and in the full-adjoint VDA are close to the true initial conditions.

Table IV provides the root-mean-squared error (RMSE) and the bias values between the true initial soil moisture profile and the model estimates for each case (dry and wet case). As illustrated in the table the lowest RMSE (bias) value for dry case is obtained by the RA-VDA approach [0.0044(9.9e-4)]. The lowest RMSE (bias) for the wet case is obtained by full adjoint [0.0065 (0.0038)], with MR-VDA having very comparable

TABLE IV
ROOT MEAN SQUARE ERROR (RMSE) AND BIAS VALUES OF ESTIMATED INITIAL SOIL MOISTURE PROFILE VERSUS TRUTH FOR BOTH DRY CASE AND WET CASE

	RMSE (Bias) [m³/m³]		
Method	Full-adjoint VDA	RA-VDA	MR-VDA
Dry case	0.0067 (0.0048)	0.0044 (9.9e-4)	0.0381 (0.0362)
Wet case	0.0065 (0.0038)	0.0111 (0.01)	0.0078 (-0.0074)

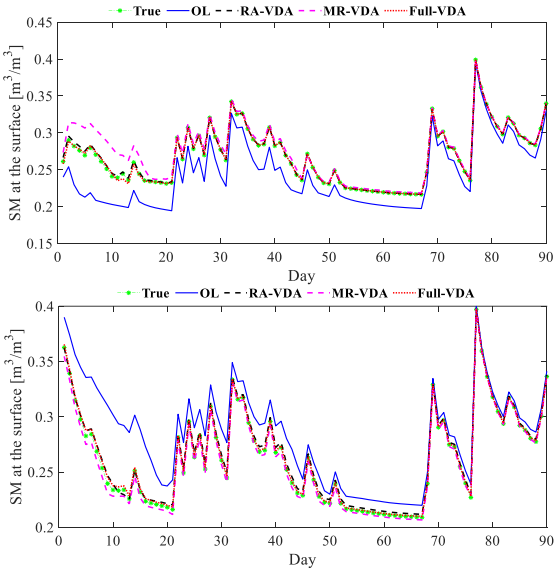

Fig. 6. Time series of estimated surface soil moisture with RA-VDA method (black), MR-VDA method (magenta), and full-adjoint VDA method (red) comparing with the surface observation (green) and open-loop simulation (blue)—dry case (top), wet case (bottom).

results. Results illustrate that RA-VDA and MR-VDA mimic the truth with acceptable RMSE and bias.

The time series of soil moisture at the surface simulated by the forward model run (Richards model) with three different retrieved initial soil moisture profiles (using full-adjoint VDA, RA-VDA, and MR-VDA) for each dry and wet case are shown in Fig. 6. For the sake of comparison, the true value of surface soil moisture observations and so-called open-loop estimates (hereafter OL) are shown as well. Note that by OL, we mean estimation of soil moisture using the forward model run described in Section II-A based on the prior values of parameters (also called initial guess) before assimilation of the surface soil moisture observations.

According to both Fig. 6 and Table V [RMSE (bias) values of simulated surface soil moisture], assimilating surface soil moisture reduces the error between the OL estimates and the truth (synthetically produced surface soil moisture) which reflects the promise of the proposed data assimilation approaches (full-adjoint VDA, RA-VDA, and MR-VDA) for soil moisture retrievals. According to Fig. 6, all three VDA methods show generally good agreement with the truth. MR-VDA overestimates the surface soil moisture for the dry case during days 1–20, as its retrieved initial soil moisture profile has been overestimated as well [Fig 5(a)]. However, the RMSE and bias values (seen in Table V) illustrate that assimilating surface soil moisture into

TABLE V
RMSE (BIAS) VALUES OF SIMULATED SURFACE SOIL MOISTURE VERSUS TRUTH FOR TWO DIFFERENT CASES, COMPARING THE RESULTS OF THREE DIFFERENT VDA APPROACHES WITH OL

	RMSE (Bias) [m^3/m^3]			
	OL	Full-adjoint VDA	RA-VDA	MR-VDA
Dry case	0.0284 (-0.0253)	0.0015 (2.3360e-04)	0.0018 (9.7838e-04)	0.0668 (-0.0302)
Wet case	0.0276 (0.0217)	0.0020 (0.0016)	0.0034 (0.0029)	0.0767 (-0.0509)

the forward model (Richards model) using MR-VDA for the dry case will compensate for the overestimated initial soil moisture profile over the simulation period. This result confirms the fact that the uncertainty related to the initial conditions will have the greatest impact (i.e., error) of the estimation of soil moisture at the beginning of assimilation period and the estimation errors decrease over time as more observations become available.

Comparison of the full-adjoint, RA-VDA, and MR-VDA results in this experiment clearly shows that the reduced-order VDA techniques (RA-VDA and MR-VDA) are promising approaches and are a comparative alternative to full-adjoint VDA for soil moisture profile estimation using surface soil moisture observations.

B. Experiment 2

In the following experiment, the performance of the proposed reduced-order VDA methods (RA-VDA and MR-VDA) using an SVAT model, such as HYDRUS-1D as the physical model is explored to demonstrate the efficiency of the reduced-order VDA techniques for estimating initial soil moisture profile in a common SVAT model. Unlike Richards model used in the first experiment, HYDRUS-1D is not easily differentiable and the computation of the adjoint of this model, needed in full-adjoint VDA, is very complex, emphasizing the importance and value of reduced-order VDA methods for estimating the soil moisture profile using variational approaches. The results from a synthetic experiment under ideal condition will be presented here. The assumption, implementation, and experiment setup is the same as experiment 1.

In order to compute PODs, forward model (HYDRUS-1D) is run with the first guess of the initial soil moisture profile and an ensemble of 90 (daily) snapshots were created. Next, the matrix P including the dominant POD modes is created capturing more than 98% of the data variability. Fig. 7 shows the increase in coverage of the variance of the data versus the number of POD modes. Having POD modes, the reduced dynamical model is created using (15).

Same as experiment 1 with Richards model as its forward model, the optimization algorithm is quasi-Newton method with BFGS updating algorithm and the convergence criteria is as shown in (21). The minimization process is completed when the change in successive cost function is too small. The performance of the reduced-order VDA methods using HYDRUS-1D as the forward model to retrieve the initial soil moisture profile is shown in Fig. 8. As it is shown in this figure, the estimated initial soil moisture profile is very close to the true initial soil

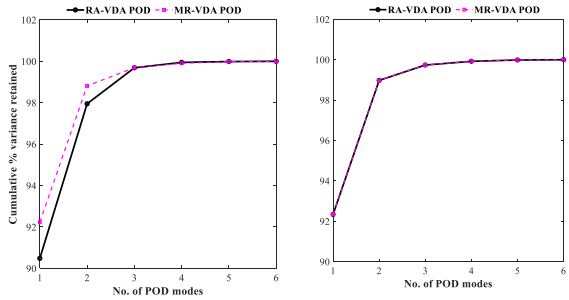

Fig. 7. Cumulative variance percentage covered by different number of POD modes, (right) dry case, and (left) wet case.

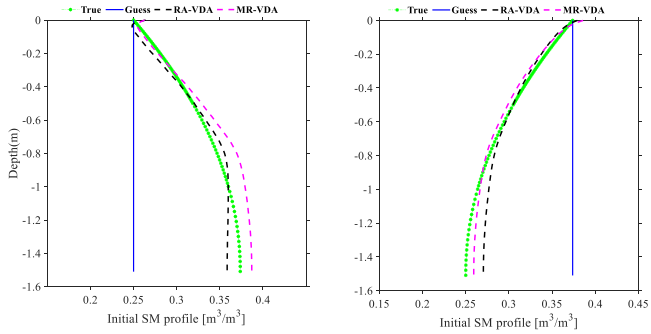

Fig. 8. Estimated initial soil moisture profile using HYDRUS-1D with RA-VDA method (black), MR-VDA method (magenta), comparing with the true (green) and initial guess (blue)—dry case (left), wet case (right).

TABLE VI
RMSE AND BIAS VALUES FOR THE INITIAL GUESS OF THE INITIAL SOIL MOISTURE PROFILE AND RETRIEVED INITIAL SOIL MOISTURE PROFILE VERSUS THE TRUTH (M^3/M^3)

RMSE (bias)	Initial guess	RA-VDA	MR-VDA
Dry case	0.0769 (-0.0668)	0.0078 (-0.0034)	0.0124 (0.0068)
Wet case	0.0824 (0.0730)	0.0092 (0.0029)	0.0061 (-0.0022)

moisture profile for each of dry and wet case. In both dry and wet cases, the estimated initial soil moisture profile closely follows the truth up to exactly 1 m below the surface and starts a slight deviation from the true at lower depth. This is potentially because the observation is only for surface soil moisture and there is no information on lower depth that can be used as the observation. It is worth noting that, according to literature [109], [110], effective root zone for most of the root-zone modeling is up to 1 m deep down the soil.

The first column of Table VI shows the RMSE and bias values between the truth and the initial guess of initial soil moisture profile. The second and third columns of the table show the RMSE and bias values between the truth and retrieved initial soil moisture profile using RA-VDA and MR-VDA. As shown in this table, the RMSE values for both RA-VDA (dry case: 0.0078 and wet case: 0.0092) and MR-VDA (dry case: 0.0068 and wet case: 0.0061) is lower than the RMSE values of the initial guess (dry case: 0.0769 and wet case: 0.0824) of soil moisture profile. Comparison between RA-VDA and MR-VDA indicates that for both dry and wet cases, the RA-VDA method reduces the RMSE in an acceptable order of magnitude. The RMSE decreases by about 90% for both the dry case and the wet case,

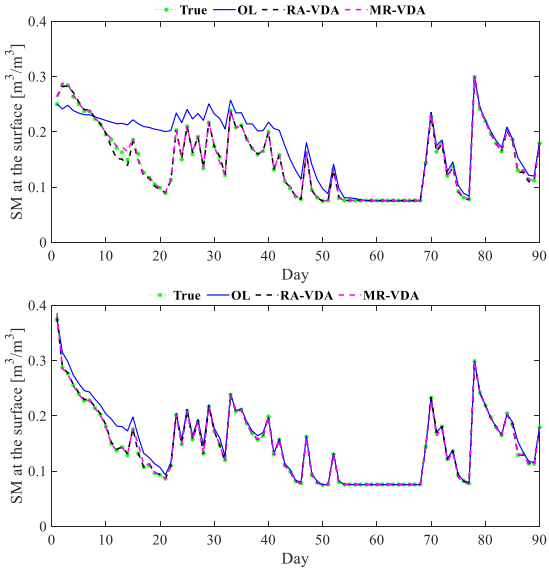

Fig. 9. Time series of estimated surface soil moisture with RA-VDA method (black), MR-VDA method (magenta), comparing with the surface observation (green) and open-loop simulation (blue)—dry case (top), wet case (bottom).

TABLE VII
RMSE AND BIAS VALUES FOR ESTIMATED SURFACE SOIL MOISTURE VERSUS THE TRUTH (M^3/M^3)

RMSE (bias)	OL	RA-VDA	MR-VDA
Dry case	0.0397 (0.0243)	0.0039 (-6.2e-4)	0.0032 (0.001)
Wet case	0.0129 (0.0069)	0.0012 (2.2e-4)	0.0027 (-1.2e-5)

while in MR-VDA the decrease in RMSE in the wet case (92%) is more than the dry case (84%). As shown in the table, for the dry case the RA-VDA method has the lowest RMSE and bias values, while for the wet case the lowest RMSE and bias values are obtained by MR-VDA. However, the difference of RMSE and bias values between MR-VDA and RA-VDA for the wet case is not significant and both perform satisfactorily.

The time series of the surface soil moisture is illustrated in Fig. 9 and the RMSE and bias values of the estimated surface soil moisture compared to the truth (i.e., synthetic true) is shown in Table VII. According to the figure, the soil moisture time series is estimated very well using RA-VDA and MR-VDA in terms of both the magnitude and day-to-day dynamics compared to the OL (i.e., simulation without any assimilation). The RMSE and bias values also decrease in an acceptable order of magnitude compared to the OL (Table VII). The results of this experiment demonstrate that a good estimation of initial soil moisture profile results in more accurate soil moisture time series simulation.

The results presented in this experiment demonstrate the efficiency and effectiveness of the proposed reduced-order VDA methods (RA-VDA and MR-VDA) in estimating initial soil moisture profile and improving the accuracy of time series of soil moisture profile by assimilating surface soil moisture observation into the highly nonlinear HYDRUS-1D model. Therefore, the important point for the interpretation of this experiment is to look at how well the model is doing in estimating the

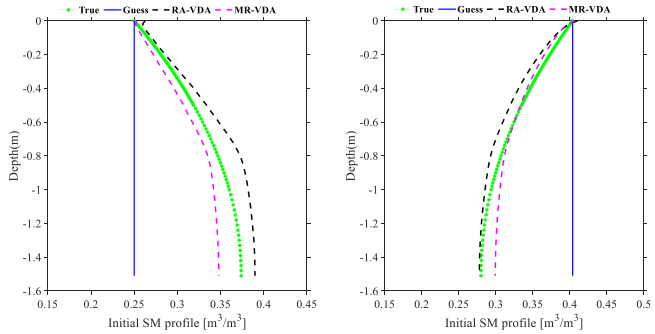

Fig. 10. Estimated initial soil moisture profile using HYDRUS-1D with RA-VDA method (black), MR-VDA method (magenta), comparing with the truth (green), and initial guess (blue)—dry case (left), wet case (right).

initial condition (e.g., initial soil moisture profile) using a highly nonlinear SVAT model, at which the computation of the adjoint of a full-adjoint VDA becomes very complex, time consuming, and even impractical. Clearly, by assimilating the surface soil moisture into HYDRUS-1D as the forward model the prior trajectories are improved and the initial soil moisture profile is estimated with a good degree of accuracy.

The next step is investigating the performance of assimilating surface soil moisture into HYDRUS-1D using the proposed assimilation algorithms (RA-VDA and MR-VDA) in order to retrieve initial soil moisture profile in conditions close to the real world under the experiments designed as follows.

C. *Experiment 3*

In this experiment, the performance of assimilating surface soil moisture into HYDRUS-1D using the proposed reduced order VDA algorithms (RA-VDA and MR-VDA) in retrieving initial soil moisture profile under nonideal (real world) conditions is investigated. The results of the experiment under different model and observational errors are presented in this section. This experiment is conducted under two scenarios. In the first scenario, the assimilation is conducted under the assumption that the physical model is perfect (i.e., known), but the observations are generated by adding random errors to the surface soil moisture obtained from the synthetic truth to consider the observation uncertainty (Section IV-C-1). In scenario 2 of this experiment, the assimilation is performed under observational and model uncertainty. Model uncertainty is taken into account by prescribing errors to weather inputs and initial conditions (Section IV-C-2).

1) Assimilation With Observation Uncertainty: In this scenario, the forcing data and the forward model is assumed known, i.e., the model uncertainty is set to zero. In order to consider the measurement error, the observations are generated by additive random perturbations (Gaussian noise with zero mean and maximum 0.03–0.04 variances) of the surface soil moisture time series. The experimental setup and the POD modes are similar to experiment 2. Fig. 10 shows the estimated initial soil moisture profile, the initial guess, and the true initial soil moisture profile in both dry and wet case. The initial guess of the initial soil moisture profile as shown in Fig. 10 is assumed to be distributed uniformly in depth, equal to the value of the surface soil

TABLE VIII
RMSE (BIAS) VALUES OF ESTIMATED INITIAL SOIL MOISTURE PROFILE VERSUS TRUTH (M^3/M^3)

RMSE (bias)	Initial guess	RA-VDA	MR-VDA
Dry case	0.0769 (-0.0668)	0.0154 (0.0136)	0.0142 (-0.0125)
Wet case	0.0824 (0.0730)	0.0123 (-0.0111)	0.0091 (0.0013)

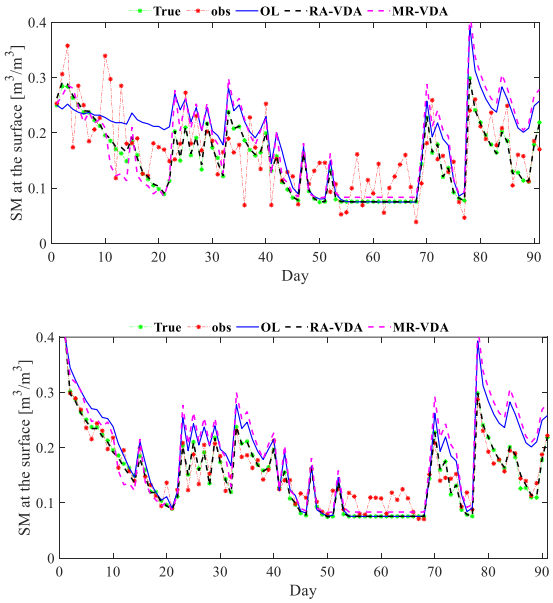

Fig. 11. Time series of estimated surface soil moisture with RA-VDA method (black), MR-VDA method (magenta), comparing with the surface observation (green) and open-loop simulation (blue) for dry case (top) and wet case (bottom).

moisture observation. As seen in Fig. 10, once the surface soil moisture is assimilated into the model, the initial soil moisture profile mimics the pattern of the true initial soil moisture profile more accurately. The RMSE and bias values of initial guess and the estimated initial soil moisture profile using both RA-VDA and MR-VDA compared to the true initial soil moisture profile is shown in Table VIII. Both RA-VDA and MR-VDA methods reduce the RMSE (bias) values compared to the initial guess of the initial soil moisture profile and are able to mimic the synthetic true soil mositure profile. Results of these two techniques are comparable and the differences are not significant in both dry and wet cases.

With the initial condition being the dominant source of uncertainty in numerical modeling of soil moisture in SVAT models (e.g., [23], [30], [34], [111], [112]), a more accurate estimate of the initial soil moisture profile would result in better estimates of the entire soil moisture time series. Fig. 11 shows the time series of surface soil moisture estimated from RA-VDA and MR-VDA and OL against the truth. As seen in these figures, the estimated soil moisture over time using both RA-VDA and MR-VDA better match the true soil moisture time series in terms of magnitude and day-to-day dynamics compared with OL. RA-VDA and MR-VDA methods significantly reduce the RMSE and bias values of the estimated surface soil moisture time series compared to the OL (as seen in Table IX) confirming the efficiency and accuracy of these techniques in retrieving the initial soil moisture profile in presence of reasonable observational error.

TABLE IX
RMSE (BIAS) VALUES OF THE ESTIMATES SURFACE SOIL MOISTURE VERSUS THE SYNTHETIC TRUE (M^3/M^3)

	RMSE (Bias)		
	OL	RA-VDA	MR-VDA
Dry case	0.0509 (0.0361)	0.0036 (0.0013)	0.0048 (-0.0018)
Wet case	0.0397 (0.0281)	0.0041 (-3.6e-4)	0.0026 (0.0012)

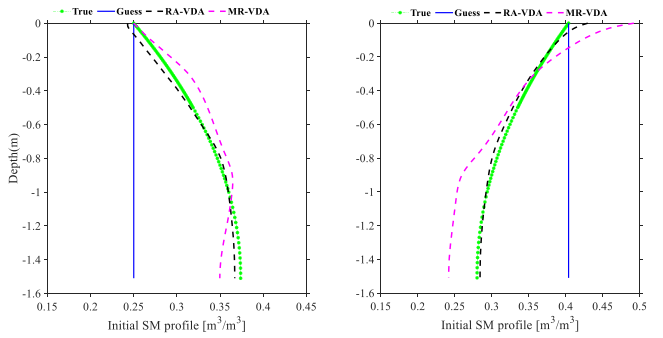

Fig. 12. Estimated initial soil moisture profile using HYDRUS-1D with RA-VDA method (black), MR-VDA method (magenta), comparing with the truth (green) and initial guess (blue)—dry case (left), wet case (right), in presence of errors.

TABLE X
RMSE VALUES OF THE ESTIMATED INITIAL SOIL MOISTURE PROFILE VERSUS THE SYNTHETIC TRUE—IN PRESENCE OF THE POSSIBLE ERRORS (M^3/M^3)

RMSE (bias)	Initial guess	RA-VDA	MR-VDA
Dry case	0.0769 (-0.0668)	0.0068 (-0.0051)	0.0140 (0.0072)
Wet case	0.0824 (0.0730)	0.0063 (-0.0015)	0.0307 (-0.0068)

2) Assimilation With Model and Observation Uncertainty: In this scenario of the experiment in addition to observational uncertainty (explained in Section IV-C-1), the modeling uncertainty is taken into account by perturbing the daily weather forcing data as described in Section III (the perturbation values is shown in Table II). Perturbations on net radiation and precipitation are multiplicative lognormally distributed with a mean of 1 and standard deviations of 3 MJ/m2d and 0.5 cm/day, respectively; perturbations on maximum and minimum temperature, humidity, and wind speed are additive Gaussian with a mean of 0 and standard deviation of 3°C, 5%, and 250 km/day, respectively. The observations are generated similar to experiment 2 by additive random perturbations to the surface soil moisture time series. Fig. 12 shows the estimated initial soil moisture profile and true initial soil moisture profile in dry and wet case. As illustrated in this figure, while the estimated initial soil moisture profile using both RA-VDA and MR-VDA mimics the truth well, RA-VDA results estimate the truth in both cases better. The calculated RMSE and bias between the estimated initial soil moisture profile using RA-VDA and MRA-VDA versus the truth and the initial guess of soil moisture profile versus the truth (Table X) confirms this observation. As observed in this table, both estimated initial soil moisture profile via RA-VDA and MR-VDA reduces the RMSE and bias values compared with the initial guess of initial soil moisture profile, used in OL calculations, with the RA-VDA method possessing a lower RMSE and bias values in comparison with the MR-VDA

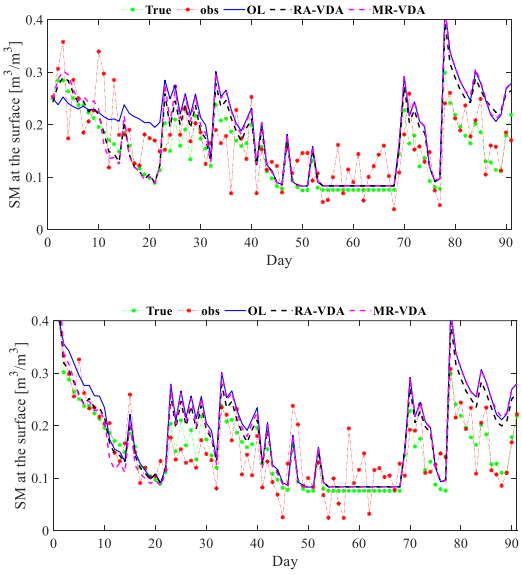

Fig. 13. Time series of estimated surface soil moisture in presence of errors with RA-VDA method (black), MR-VDA method (magenta), comparing with the surface observation (green) and open-loop simulation (blue) for dry case (top) and wet case (bottom).

method. The results here are obtained by assuming that both the model and observation are not perfect and have errors.

Once the initial soil moisture profile is retrieved, the soil moisture time series is simulated with higher degree of accuracy. The estimated surface soil moisture time series, the observation, the true surface soil moisture, and the OL are shown in Fig. 13. As seen in these figures, the simulated surface soil moisture using the retrieved initial soil moisture profile, for both RA-VDA and MR-VDA and both dry case and wet case, generally matches the truth and accurately estimates day-to-day dynamics of the surface soil moisture observations. However, when the precipitation error is high, deviation between the estimated soil moisture and the truth increases. One possible reason is related to the role of the relation between the precipitation rate and the saturated hydraulic conductivity (K_{sat}) in defining the surface runoff. For example, at day 80, the truth precipitation is 7.97 cm/day ($<K_{\mathrm{sat}}$ of 13.19 cm/day), and the observed precipitation (i.e., with added error) is 14.85 ($>K_{\mathrm{sat}}$ of 13.19 cm/day). Therefore, the OL and the reduced-order VDA's will operate under the assumption that surface runoff occurs (since, precipitation $>$ K_{sat}), while in the truth system there is no runoff ($P < K_{\mathrm{sat}}$). In this case, the negative impact of model error/uncertainty (in the form of forcing error) overshadows the improvements resulting from more accurate initial soil moisture conditions (as seen in the figure). Reichle *et al.* [113] and Das and Mohanty [114] also reported on the significant impact of the precipitation on the soil moisture estimates. Among the entire model inputs, the precipitation is the one that most dominates soil moisture, and at the same time, it is also the input with the highest uncertainty.

Table XI illustrates the RMSE values of surface soil moisture for OL, RA-VDA, and MR-VDA compared to the truth. As indicated, the RMSE and bias values decreased compared with the OL, but since the model has error, the values are not too small. The values of RMSE and bias in both dry and wet cases

TABLE XI
RMSE VALUES OF THE SURFACE SOIL MOISTURE VERSUS THE SYNTHETIC TRUE (M^3/M^3)

RMSE (Bias)	OL	RA-VDA	MR-VDA
Dry case	0.0562 (0.0408)	0.0407 (0.0254)	0.0481 (0.0307)
Wet case	0.0511 (0.0370)	0.0393 (0.0261)	0.0502 (0.0310)

are lower when RA-VDA method is used. It is concluded from the results that RA-VDA method performs well in retrieving the initial soil moisture profile by assimilating the soil moisture observations into a highly nonlinear SVAT model in presence of error by mimicking real world observational and forcing errors.

V. CONCLUSION

In this article, full-adjoint VDA and two reduced-order VDAs (MR-VDA and RA-VDA) are investigated to retrieve the initial soil moisture profile from surface soil moisture observations. Reduced-order VDA approaches not only avoid the complex implementation of the adjoint model, but are also computationally more efficient as compared to the full-adjoint VDA. In the MR-VDA, the adjoint model is approximated based on the reduced-order model, and the entire optimization is performed in a reduced space. However, in the RA-VDA, only the adjoint is computed in the reduced space and the optimization is conducted on the original space. In this article, both full-adjoint VDA and reduced-order VDA (both RA-VDA and MR-VDA) are used to retrieve the initial soil moisture profile of a 1-D soil water balance model using surface soil moisture observations.

In order to address the questions and objectives of this article, a set of synthetic experiments is conducted. The feasibility and accuracy of the proposed VDA approaches in estimating the initial soil moisture profile from implicit information contained in time series of surface soil moisture observations are explored in experiment 1. To focus on the accuracy of the variational approaches in retrieving the initial soil moisture profile, the assimilation is operated under ideal condition. Ideal condition here means the same physical model, the same model inputs, and the same error statistics are used for the generation of the synthetic true surface soil moisture in both the observation and the assimilation process. Although the results of the experiments in ideal conditions are unrealistically good, such experiments will give us confidence in the performance of the algorithm. Therefore, the important point for the interpretation of such experiment is to look at how well the proposed VDA approaches are doing in estimating the initial condition. In experiment 1, full-adjoint VDA and reduced-order VDA (RA-VDA and MR-VDA) were implemented on Richards model. The results of this experiment lead to the conclusion that VDA approaches can significantly improve the prior trajectories and are able to estimate the initial soil moisture profile with a good degree of accuracy. In addition, it is concluded that the results of RA-VDA and MR-VDA have higher convergence rate (lower number of iterations) and less complexity compared to full-adjoint VDA. Moreover, both RA-VDA and MR-VDA are more efficient in terms of computational cost since in each iteration, the forward model run in MR-VDA and backward model run in both

MR-VDA and RA-VDA are in reduced space. While in the full-adjoint VDA, both forward and backward model run are in the full space.

Next, experiment 2 is designed under ideal condition in order to test and illustrate the efficiency of the proposed reduced-order VDA techniques in estimating initial soil moisture profile by assimilating surface soil moisture observations into highly nonlinear SVAT models such as HYDRUS-1D. The results of this experiment show that while both RA-VDA and MR-VDA methods are able to retrieve the initial soil moisture profile by assimilating surface soil moisture observation into an SVAT model, RA-VDA has slightly better results in both dry and wet soil moisture conditions.

To further investigate the performance of the proposed reduced-order VDA approaches in estimation of soil moisture profile in presence of error mimicking real world observational and forcing errors, experiment 3 is conducted under nonideal condition. Nonideal condition means different inputs and statistics are used in both the synthetic truth and the estimation process. To this end, experiment 3 is employed under two different scenarios. The assimilation algorithm in the first scenario is investigated under the condition when the physical model is exactly known, but the observations are generated by adding random errors to the surface soil moisture obtained from the synthetic truth to consider observation uncertainty. In scenario 2, the assimilation algorithm is performed by prescribing errors to weather inputs and initial conditions to account for model uncertainty in addition to the observation uncertainty. The results under both scenarios show that retrieved initial soil moisture profile using both RA-VDA and MR-VDA approaches are comparable, with RA-VDA slightly outperforming MR-VDA.

The results of the three experiments performed in this article demonstrate that the RA-VDA method has comparable results with full-adjoint VDA and slightly better results than MR-VDA and is able to accurately retrieve the initial soil moisture profile in all synthetic experiments at very reasonable computation cost. Even though we made an effort to mimic realistic conditions, there can be no guarantee that the results remain completely unchanged if we use satellite measurements and reanalysis meteorological data to apply the proposed approaches on a large-scale application. The method has yet to be verified with a number of real field-areal datasets in the large-scale experiment. If successful, the approach may contribute to the improvement of the representation of land surface hydrology at regional scales. To assess the general usefulness of the reduced-order VDA method at operational scales of land surface modeling, additional tests and further considerations in a watershed scale and using spaceborne data in presence of unknown soil hydraulic parameters (not addressed in this article) would be required. Hence, our future article will focus on 1) expanding the reduced-order VDA approaches, namely RA-VDA to estimate soil hydraulic parameters in addition to initial soil moisture profile by assimilating surface soil moisture observations into SVAT models (e.g., HYDRUS-1D), and 2) testing the feasibility of the RA-VDA method for estimating soil hydraulic parameter and soil moisture profile estimation using remotely sensed surface soil moisture observations.

SUPPLEMENTARY

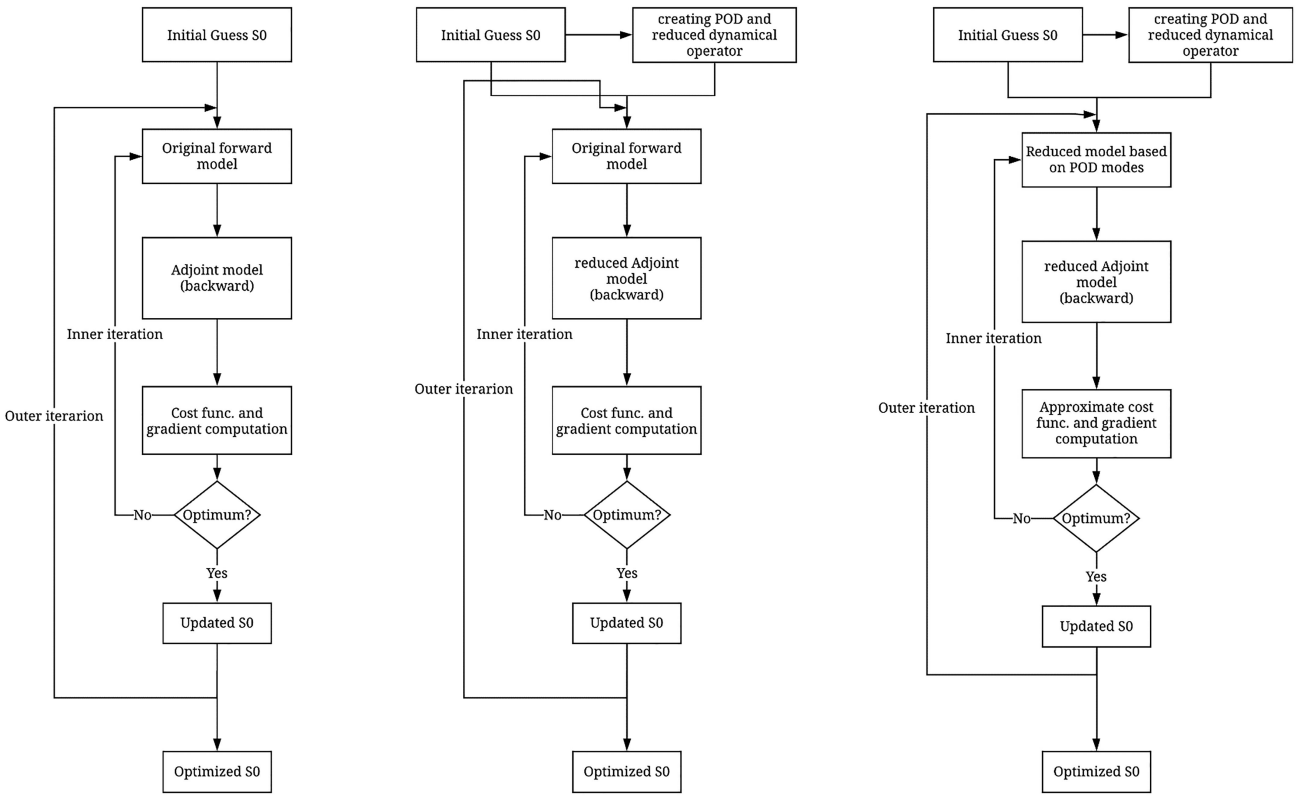

Fig. S1. Flowcharts of initial soil moisture profile (S0) estimation using full-adjoint VDA (left), RA-VDA (middle) and MR-VDA (right) POD: Proper Orthogonal Decomposition.

REFERENCES

[1] J. A. Santanello *et al.*, "Using remotely-sensed estimates of soil moisture to infer soil texture and hydraulic properties across a semi-arid watershed," *Remote Sens. Environ.*, vol. 110, no. 1, pp. 79–97, Sep. 2007.

[2] C. Montzka, H. Moradkhani, L. Weihermüller, H. J. H. Franssen, M. Canty, and H. Vereecken, "Hydraulic parameter estimation by remotely-sensed top soil moisture observations with the particle filter," *J. Hydrol.*, vol. 399, no. 3/4, pp. 410–421, 2011.

[3] J. Li and S. Islam, "On the estimation of soil moisture profile and surface fluxes partitioning from sequential assimilation of surface layer soil moisture," *J. Hydrol.*, vol. 220, no. 1/2, pp. 86–103, 1999.

[4] J. Van Der Kruk, C. M. Steelman, A. L. Endres, and H. Vereecken, "Dispersion inversion of electromagnetic pulse propagation within freezing and thawing soil waveguides," *Geophys. Res. Lett.*, vol. 36, pp. 2–5, 2009.

[5] M. Zreda, D. Desilets, T. P. A. Ferre, and R. L. Scott, "Measuring soil moisture content non-invasively at intermediate spatial scale using cosmic-ray neutrons," *Geophys. Res. Lett.*, vol. 35, pp. 1–5, 2008.

[6] J. P. Grant, J.-P. Wigneron, A. A. Van de Griend, A. Kruszewski, S. S. Søbjærg, and N. Skou, "A field experiment on microwave forest radiometry: L-band signal behaviour for varying conditions of surface wetness," *Remote Sens. Environ.*, vol. 109, no. 1, pp. 10–19, 2007.

[7] C. Oberdörster, J. Vanderborght, A. Kemna, and H. Vereecken, "Investigating preferential flow processes in a forest soil using time domain reflectometry and electrical resistivity tomography," *Vadose Zone J.*, vol. 9, no. 2, pp. 350–361, May 2010.

[8] I. Hajnsek, T. Jagdhuber, H. Schön, and K. P. Papathanassiou, "Potential of estimating soil moisture under vegetation cover by means of PolSAR," *IEEE Trans. Geosci. Remote Sens.*, vol. 47, no. 2, pp. 442–454, Feb. 2009.

[9] K. Saleh *et al.*, "Soil moisture retrievals at L-band using a two-step inversion approach (COSMOS/NAFE'05 experiment)," *Remote Sens. Environ.*, vol. 113, no. 6, pp. 1304–1312, Jun. 2009.

[10] S. Paloscia, G. Macelloni, and E. Santi, "Soil moisture estimates from AMSR-E brightness temperatures by using a dual-frequency algorithm," *IEEE Trans. Geosci. Remote Sens.*, vol. 44, no. 11, pp. 3135–3144, Nov. 2006.

[11] W. Wagner, K. Scipal, C. Pathe, D. Gerten, W. Lucht, and B. Rudolf, "Evaluation of the agreement between the first global remotely sensed soil moisture data with model and precipitation data," *J. Geophys. Res. Atmos.*, vol. 108, no. 19, 2003, Art. no. 4611.

[12] L. Brocca, F. Melone, T. Moramarco, W. Wagner, and S. Hasenauer, "ASCAT soil wetness index validation through in situ and modeled soil moisture data in central Italy," *Remote Sens. Environ.*, vol. 114, no. 11, pp. 2745–2755, 2010.

[13] F. Li, W. T. Crow, and W. P. Kustas, "Towards the estimation root-zone soil moisture via the simultaneous assimilation of thermal and microwave soil moisture retrievals," *Adv. Water Resour.*, vol. 33, no. 2, pp. 201–214, 2010.

[14] N. Baghdadi, N. Holah, and M. Zribi, "Soil moisture estimation using multi-incidence and multi-polarization ASAR data," *Int. J. Remote Sens.*, vol. 27, no. 10, pp. 1907–1920, 2006.

[15] M. Takada, Y. Mishima, and S. Natsume, "Estimation of surface soil properties in peatland using ALOS/PALSAR," *Landscape Ecol. Eng.*, vol. 5, no. 1, pp. 45–58, 2009.

[16] Y. H. Kerr, P. Waldteufel, J.-P. Wigneron, J. Martinuzzi, J. Font, and M. Berger, "Soil moisture retrieval from space: The soil moisture and ocean salinity (SMOS) mission," *IEEE Trans. Geosci. Remote Sens.*, vol. 39, no. 8, pp. 1729–1735, Aug. 2001.

[17] D. Entekhabi *et al.*, "The soil moisture active passive (SMAP) mission," *Proc. IEEE*, vol. 98, no. 5, pp. 704–716, May 2010.

[18] D. Enrekhabi *et al.*, "SMAP handbook: Mapping soil moisture and freeze/thaw from space," *JPL Publ.*, pp. 400–1567, 2014.

[19] H. Vereecken, J. A. Huisman, H. Bogena, J. Vanderborght, J. A. Vrugt, and J. W. Hopmans, "On the value of soil moisture measurements in vadose zone hydrology: A review," *Water Resour. Res.*, vol. 44, no. 4, Apr. 2008, doi: 10.1029/2008WR006829.

[20] R. Ruggenthaler, G. Meißl, C. Geitner, G. Leitinger, N. Endstrasser, and F. Schöberl, "Investigating the impact of initial soil moisture conditions on total infiltration by using an adapted double-ring infiltrometer," *Hydrol. Sci. J.*, vol. 61, pp. 1–17, Mar. 2016.

[21] C. Fitzjohn, J. L. Ternan, and A. G. Williams, "Soil moisture variability in a semi-arid gully catchment: Implications for runoff and erosion control," *CATENA*, vol. 32, no. 1, pp. 55–70, 1998.

[22] H. Liu, T. W. Lei, J. Zhao, C. P. Yuan, Y. T. Fan, and L. Q. Qu, "Effects of rainfall intensity and antecedent soil water content on soil infiltrability under rainfall conditions using the run off-on-out method," *J. Hydrol.*, vol. 396, no. 1/2, pp. 24–32, Jan. 2011.

[23] V. M. Castillo, A. Gómez-Plaza, and M. Martıńez-Mena, "The role of antecedent soil water content in the runoff response of semiarid catchments: A simulation approach," *J. Hydrol.*, vol. 284, no. 1, pp. 114–130, 2003.

[24] A. Cerdà, "Seasonal variability of infiltration rates under contrasting slope conditions in southeast Spain," *Geoderma*, vol. 69, no. 3, pp. 217–232, 1996.

[25] A. Cerdà, "Seasonal changes of the infiltration rates in a mediterranean scrubland on limestone," *J. Hydrol.*, vol. 198, no. 1, pp. 209–225, 1997.

[26] E. Meyles, A. Williams, L. Ternan, and J. Dowd, "Runoff generation in relation to soil moisture patterns in a small dartmoor catchment, Southwest England," *Hydrol. Process.*, vol. 17, no. 2, pp. 251–264, Feb. 2003.

[27] E. Zehe, R. Becker, A. Bárdossy, and E. Plate, "Uncertainty of simulated catchment runoff response in the presence of threshold processes: Role of initial soil moisture and precipitation," *J. Hydrol.*, vol. 315, no. 1–4, pp. 183–202, 2005.

[28] L. Berthet and V. Andr, "How crucial is it to account for the antecedent moisture conditions in flood forecasting ? Comparison of event-based and continuous approaches on 178 catchments," *Hydrol. Syst. Sci.*, vol. 13, pp. 819–831, 2009.

[29] L. Brocca, F. Melone, T. Moramarco, and V. P. Singh, "Assimilation of observed soil moisture data in storm rainfall-runoff modeling," *J. Hydrol. Eng.*, vol. 14, no. 2, pp. 153–165, 2009.

[30] M. G. Grillakis, A. G. Koutroulis, J. Komma, I. K. Tsanis, W. Wagner, and G. Blöschl, "Initial soil moisture effects on flash flood generation—A comparison between basins of contrasting hydro-climatic conditions," *J. Hydrol.*, vol. 541, pp. 206–217, 2016.

[31] M. Huang, J. Gallichand, C. Dong, Z. Wang, and M. Shao, "Use of soil moisture data and curve number method for estimating runoff in the loess plateau of China," *Hydrol. Process.*, vol. 21, no. 11, pp. 1471–1481, May 2007.

[32] M. Le Lay and G. M. Saulnier, "Exploring the signature of climate and landscape spatial variabilities in flash flood events: Case of the 8–9 September 2002 Cévennes-vivarais catastrophic event," *Geophys. Res. Lett.*, vol. 34, 2007, Art. no. L13401, doi: 10.1029/2007GL029746.

[33] H. Li, M. Sivapalan, and F. Tian, "Comparative diagnostic analysis of runoff generation processes in Oklahoma DMIP2 basins: The Blue river and the Illinois river," *J. Hydrol.*, vol. 418/419, pp. 90–109, 2012.

[34] C. Massari, L. Brocca, T. Moramarco, Y. Tramblay, and J.-F. D. Lescot, "Potential of soil moisture observations in flood modelling: Estimating initial conditions and correcting rainfall," *Adv. Water Resour.*, vol. 74, pp. 44–53, 2014.

[35] C. Massari, L. Brocca, S. Barbetta, C. Papathanasiou, M. Mimikou, and T. Moramarco, "Using globally available soil moisture indicators for flood modelling in mediterranean catchments," *Hydrol. Earth Syst. Sci.*, vol. 18, no. 2, pp. 839–853, Feb. 2014.

[36] C. Massari *et al.*, "The use of H-SAF soil moisture products for operational hydrology: Flood modelling over Italy," *Hydrology*, vol. 2, no. 1, pp. 2–22, 2015.

[37] Y. Tramblay *et al.*, "Estimation of antecedent wetness conditions for flood modelling in northern Morocco," *Hydrol. Earth Syst. Sci.*, vol. 16, no. 11, pp. 4375–4386, Nov. 2012.

[38] Y. Tramblay, C. Bouvier, C. Martin, J.-F. Didon-Lescot, D. Todorovik, and J.-M. Domergue, "Assessment of initial soil moisture conditions for event-based rainfall–runoff modelling," *J. Hydrol.*, vol. 387, no. 3/4, pp. 176–187, Jun. 2010.

[39] A. C. M. Beljaars, P. Viterbo, M. J. Miller, and A. K. Betts, "The anomalous rainfall over the United States during July 1993: Sensitivity to land surface parameterization and soil moisture anomalies," *Monthly Weather Rev.*, vol. 124, no. 3, pp. 362–383, Mar. 1996.

[40] R. D. Koster *et al.*, "The second phase of the global land-atmosphere coupling experiment: Soil moisture contributions to subseasonal forecast skill," *J. Hydrometeorol.*, vol. 12, no. 5, pp. 805–822, 2011.

[41] H. Zhang and C. S. Frederiksen, "Local and nonlocal impacts of soil moisture initialization on AGCM seasonal forecasts: A model sensitivity study," *J. Clim.*, vol. 16, no. 13, pp. 2117–2137, 2003.

[42] P. R. Houser, W. J. Shuttleworth, J. S. Famiglietti, H. V. Gupta, K. H. Syed, and D. C. Goodrich, "Integration of soil moisture remote sensing and hydrologic modeling using data assimilation," *Water Resour. Res.*, vol. 34, no. 12, pp. 3405–3420, Dec. 1998.

[43] M. S. Moran, C. D. Peters-Lidard, J. M. Watts, and S. Mc Elroy, "Estimating soil moisture at the watershed scale with satellite-based radar and land surface models," *Can. J. Remote Sens.*, vol. 30, no. 5, pp. 805–826, 2004.

[44] K. G. Kostov and T. J. Jackson, "Estimating profile soil moisture from surface-layer measurements: A review," *Ground Sens.*, vol. 1941, pp. 125–136, Aug. 1993.

[45] R. H. Reichle, *Variational Assimilation of Remote Sensing Data for Land Surface Hydrologic Applications*. Cambridge, MA, USA: Massachusetts Inst. Technol., 2000.

[46] J. S. Pelc, E. Simon, L. Bertino, G. El Serafy, and A. W. Heemink, "Application of model reduced 4D-Var to a 1D ecosystem model," *Ocean Model*, vol. 57–58, pp. 43–58, 2012.

[47] M. U. Altaf, M. Ambrozic, M. F. McCabe, and I. Hoteit, "A study of reduced-order 4DVAR with a finite element shallow water model," *Int. J. Numer. Methods Fluids*, vol. 80, no. 11, pp. 631–647, Apr. 2016.

[48] N. Brandhorst, D. Erdal, and I. Neuweiler, "Soil moisture prediction with the ensemble kalman filter: Handling uncertainty of soil hydraulic parameters," *Adv. Water Resour.*, vol. 110, pp. 360–370, Dec. 2017.

[49] G. J. M. De Lannoy, R. H. Reichle, P. R. Houser, V. R. N. Pauwels, and N. E. C. Verhoest, "Correcting for forecast bias in soil moisture assimilation with the ensemble Kalman filter," *Water Resour. Res.*, vol. 43, no. 9, Sep. 2007, doi: 10.1029/2006WR005449.

[50] J. Dong, S. C. Steele-Dunne, T. E. Ochsner, and N. van de Giesen, "Determining soil moisture by assimilating soil temperature measurements using the ensemble kalman filter," *Adv. Water Resour.*, vol. 86, pp. 340–353, Aug. 2015.

[51] D. Entekhabi and E. G. Njoku, "Solving the inverse problem for soil moisture and temperature profiles by sequential assimilation of multifrequency remotely sensed observations," *IEEE Trans. Geosci. Remote Sens.*, vol. 32, no. 2, pp. 438–448, Mar. 1994.

[52] J. F. Galantowicz, D. Entekhabi, and E. G. Njoku, "Tests of sequential data assimilation for retrieving profile soil moisture and temperature from observed L-band radiobrightness," *IEEE Trans. Geosci. Remote Sens.*, vol. 37, no. 4, pp. 1860–1870, Jul. 1999.

[53] C. Huang, X. Li, and L. Lu, "Retrieving soil temperature profile by assimilating MODIS LST products with ensemble Kalman filter," *Remote Sens. Environ.*, vol. 112, pp. 1320–1336, 2008.

[54] H. Moradkhani, S. Sorooshian, H. V. Gupta, and P. R. Houser, "Dual state-parameter estimation of hydrological models using ensemble Kalman filter," *Adv. Water Resour.*, vol. 28, no. 2, pp. 135–147, 2005.

[55] V. R. N. Pauwels, N. E. C. Verhoest, G. J. M. De Lannoy, V. Guissard, C. Lucau, and P. Defourny, "Optimization of a coupled hydrology-crop growth model through the assimilation of observed soil moisture and leaf area index values using an ensemble Kalman filter," *Water Resour. Res.*, vol. 43, no. 4, pp. 1–17, 2007.

[56] R. H. Reichle, D. B. McLaughlin, and D. Entekhabi, "Hydrologic data assimilation with the ensemble kalman filter," *Monthly Weather Rev.*, vol. 130, no. 1, pp. 103–114, 2002.

[57] Y. Zhou, D. McLaughlin, and D. Entekhabi, "Assessing the performance of the ensemble kalman filter for land surface data assimilation," *Monthly Weather Rev.*, vol. 134, no. 8, pp. 2128–2142, Aug. 2006.

[58] G. Evensen, "Sequential data assimilation with a nonlinear quasi-geostrophic model using Monte Carlo methods to forecast error statistics," *J. Geophys. Res.*, vol. 99, no. C5, pp. 10143–10162, May 1994.

[59] R. H. Reichle, R. D. Koster, P. Liu, S. P. P. Mahanama, E. G. Njoku, and M. Owe, "Comparison and assimilation of global soil moisture retrievals from the advanced microwave scanning radiometer for the earth observing system (AMSR-E) and the scanning multichannel microwave radiometer (SMMR)," *J. Geophys. Res. Atmos.*, vol. 112, no. 9, May 2007.

[60] A. Abdolghafoorian and L. Farhadi, "Uncertainty quantification in land surface hydrologic modeling: Toward an integrated variational data assimilation framework," *IEEE J. Sel. Topics Appl. Earth Observ. Remote Sens.*, vol. 9, no. 6, pp. 2628–2637, Jun. 2016.

[61] H. Moradkhani, "Hydrologic remote sensing and land surface data assimilation," *Sensors*, vol. 8, no. 5, pp. 2986–3004, 2008.

[62] A. H. Jazwinski, *Stochastic Processes and Filtering Theory*. Chelmsford, MA, USA: Courier Corporation, 2007.

[63] P. T. M. Vermeulen and A. W. Heemink, "Model-reduced variational data assimilation," *Monthly Weather Rev.*, vol. 134, no. 10, pp. 2888–2899, Oct. 2006.

[64] L. Ljung, "Asymptotic behavior of the extended kalman filter as a parameter estimator for linear systems," *IEEE Trans. Autom. Control*, vol. 24, no. 1, pp. 36–50, Feb. 1979.

[65] A. W. Heemink, E. E. A. Mouthaan, M. R. T. Roest, E. A. H. Vollebregt, K. B. Robaczewska, and M. Verlaan, "Inverse 3D shallow water flow modelling of the continental shelf," *Continent Shelf Res.*, vol. 22, no. 3, pp. 465–484, Feb. 2002.

[66] R. W. Lardner and Y. Song, "Optimal estimation of eddy viscosity and friction coefficients for a quasi-three-dimensional numerical tidal model," *Atmos.-Ocean*, vol. 33, no. 3, pp. 581–611, Sep. 1995.

[67] D. S. Ullman and R. E. Wilson, "Model parameter estimation from data assimilation modeling: Temporal and spatial variability of the bottom drag coefficient," *J. Geophys. Res. Ocean.*, vol. 103, no. C3, pp. 5531–5549, Mar. 1998.

[68] R. H. Reichle, D. B. McLaughlin, and D. Entekhabi, "Variational data assimilation of microwave radiobrightness observations for land surface hydrology applications," *IEEE Trans. Geosci. Remote Sens.*, vol. 39, no. 8, pp. 1708–1718, Aug. 2001.

[69] Y. Cao, J. Zhu, I. M. Navon, and Z. Luo, "A reduced-order approach to four-dimensional variational data assimilation using proper orthogonal decomposition," *Int. J. Numer. Methods Fluids*, vol. 53, no. 10, pp. 1571–1583, Apr. 2007.

[70] I. Hoteit and A. Köhl, "Efficiency of reduced-order, time-dependent adjoint data assimilation approaches," *J. Oceanogr.*, vol. 62, no. 4, pp. 539–550, 2006.

[71] A. Abdolghafoorian, L. Farhadi, S. M. Bateni, S. Margulis, and T. Xu, "Characterizing the effect of vegetation dynamics on the bulk heat transfer coefficient to improve variational estimation of surface turbulent fluxes," *J. Hydrometeorol.*, vol. 18, no. 2, pp. 321–333, 2017.

[72] A. Abdolghafoorian and L. Farhadi, "Estimation of surface turbulent fluxes from land surface moisture and temperature via a variational data assimilation framework," *Water Resour. Res.*, vol. 55, no. 6, pp. 4648–4667, 2019.

[73] A. Abdolghafoorian and L. Farhadi, "LIDA: A land integrated data assimilation framework for mapping land surface heat and evaporative fluxes by assimilating space-borne soil moisture and land surface temperature," *Water Resour. Res.*, vol. 56, no. 8, pp. 1–19, 2020.

[74] A. Griewank, "Achieving logarithmic growth of temporal and spatial complexity in reverse automatic differentiation," *Optim. Methods Softw.*, vol. 1, no. 1, pp. 35–54, Jan. 1992.

[75] G. Corliss, C. Faure, A. Griewank, L. Hascoet, and U. Naumann, *Automatic Differentiation: From Simulation to Optimization*. New York, NY, USA: Springer-Verlag, 2001.

[76] I. Hoteit, B. Cornuelle, V. Thierry, and D. Stammer, "Impact of resolution and optimized ECCO forcing on simulations of the tropical pacific," *J. Atmos. Ocean. Technol.*, vol. 25, no. 1, pp. 131–147, Jan. 2008.

[77] T. Kaminski, R. Giering, M. Scholze, P. Rayner, and W. Knorr, "An example of an automatic differentiation-based modelling system," in *Proc. Int. Conf. Comput. Sci. Appl.*, 2003, pp. 95–104.

[78] M. U. Altaf, M. El Gharamti, A. W. Heemink, and I. Hoteit, "A reduced adjoint approach to variational data assimilation," *Comput. Methods Appl. Mech. Eng.*, vol. 254, pp. 1–13, 2013.

[79] P. Courtier, J.-N. Thépaut, and A. Hollingsworth, "A strategy for operational implementation of 4D-Var, using an incremental approach," *Quart. J. Roy. Meteorol. Soc.*, vol. 120, no. 519, pp. 1367–1387, Jul. 1994.

[80] A. Schiller and J. Willebrand, "A technique for the determination of surface heat and freshwater fluxes from hydrographic observations, using an approximate adjoint ocean circulation model," *J. Mar. Res.*, vol. 53, no. 3, pp. 433–451, May 1995.

[81] A. S. Lawless, N. K. Nichols, C. Boess, and A. Bunse-Gerstner, "Using model reduction methods within incremental four-dimensional variational data assimilation," *Monthly Weather Rev.*, vol. 136, no. 4, pp. 1511–1522, Apr. 2008.

[82] A. C. Antoulas, *Approximation of Large-Scale Dynamical Systems*. Philadelphia, PA, USA: Soc. for Ind. Appl. Math., 2005.

[83] M. U. Altaf, M. Verlaan, and A. W. Heemink, "Efficient identification of uncertain parameters in a large-scale tidal model of the European continental shelf by proper orthogonal decomposition," *Int. J. Numer. Methods Fluids*, vol. 68, no. 4, pp. 422–450, Feb. 2012.

[84] M. U. Altaf, A. W. Heemink, M. Verlaan, and I. Hoteit, "Simultaneous perturbation stochastic approximation for tidal models," *Ocean Dyn.*, vol. 61, no. 8, pp. 1093–1105, 2011.

[85] M. P. Kaleta, R. G. Hanea, A. W. Heemink, and J.-D. Jansen, "Model-reduced gradient-based history matching," *Comput. Geosci.*, vol. 15, no. 1, pp. 135–153, Jan. 2011.

[86] M. U. Altaf, *Model Reduced Variational Data Assimilation for Shallow Water Flow Models*. Delft, The Netherlands: Delft Univ. Technol., 2011.

[87] G. S. Nearing, W. T. Crow, K. R. Thorp, M. S. Moran, R. H. Reichle, and H. V. Gupta, "Assimilating remote sensing observations of leaf area index and soil moisture for wheat yield estimates: An observing system simulation experiment," *Water Resour. Res.*, vol. 48, pp. 1–13, 2012.

[88] L. A. Richards, "Capillary conduction of liquids through porous mediums," *Physics*, vol. 1, no. 5, pp. 318–333, Nov. 1931.
[89] C.-T. Lai and G. Katul, "The dynamic role of root-water uptake in coupling potential to actual transpiration," *Adv. Water Resour.*, vol. 23, no. 4, pp. 427–439, Jan. 2000.
[90] X. Zeng and M. Decker, "Improving the numerical solution of soil moisture-based Richards equation for land models with a deep or shallow water table," *J. Hydrometeorol.*, vol. 10, no. 1, pp. 308–319, 2009.
[91] F. H. Fashi, M. Gorji, and M. Shorafa, "Estimation of soil hydraulic parameters for different land-uses," *Model. Earth Syst. Environ.*, vol. 2, no. 4, 2016, Art. no. 170.
[92] M. T. van, G. J. Šimůnek, M. Šejna, H. Saito, and M. Sakai, *The HYDRUS-1D Software Package for Simulating the One-Dimensional Movement of Water, Heat, and Multiple Solutes in Variably-Saturated Media*. Riverside, California, USA: Dept. Environment. Sci., Univ. California Riverside, pp. 342, 2013.
[93] J. C. van Dam and R. A. Feddes, "Numerical simulation of infiltration, evaporation and shallow groundwater levels with the Richards equation," *J. Hydrol.*, vol. 233, no. 1–4, pp. 72–85, Jun. 2000.
[94] R. H. Brooks and A. T. Corey, *Hydraulic Properties of Porous Media*. Fort Collins, CO, USA: Colorado State Univ. Libraries, 1964.
[95] R. B. Clapp and G. M. Hornberger, "Empirical equations for some soil hydraulic properties," *Water Resour. Res.*, vol. 14, no. 4, pp. 601–604, Aug. 1978.
[96] J. Simunek, M. T. Van Genuchten, and M. Sejna, "The HYDRUS-1D software package for simulating the one-dimensional movement of water, heat, and multiple solutes in variably-saturated media," *Univ. California-Riverside Res. Rep.*, vol. 3, pp. 1–240, 2005.
[97] M. T. van Genuchten, "A closed-form equation for predicting the hydraulic conductivity of unsaturated soils," *Soil Sci. Soc. Amer. J.*, vol. 44, no. 5, pp. 892–898, Sep. 1980.
[98] F.-X. L. Dimet and O. Talagrand, "Variational algorithms for analysis and assimilation of meteorological observations: Theoretical aspects," *Tellus A Dyn. Meteorol. Oceanogr.*, vol. 38, no. 2, pp. 97–110, Jan. 1986.
[99] W. C. Thacker, "Fitting models to inadequate data by enforcing spatial and temporal smoothness," *J. Geophys. Res.*, vol. 93, no. C9, pp. 10655, 1988, doi: 10.1029/JC093iC09p10655.
[100] L. Sirovich, "Turbulence and the dynamics of coherent structures. III. Dynamics and scaling," *Quart. Appl. Math.*, vol. 45, no. 3, pp. 583–590, 1987.
[101] W. H. A. Schilders, H. A. Van der Vorst, and J. Rommes, *Model Order Reduction: Theory, Research Aspects and Applications*, Cham, Switzerland: Springer, 2008.
[102] I. Hoteit and A. Köhl, "Efficiency of reduced-order, time-dependent adjoint data assimilation approaches," *J. Oceanogr.*, vol. 62, no. 4, pp. 539–550, Aug. 2006.
[103] P. J. Sellers, F. G. Hall, G. Asrar, D. E. Strebel, and R. E. Murphy, "An overview of the first international satellite land surface climatology project (ISLSCP) field experiment (FIFE)," *J. Geophys. Res. Atmos.*, vol. 97, no. D17, pp. 18345–18371, Nov. 1992.
[104] R. G. Allen, L. S. Pereira, D. Raes, and M. Smith, *Crop Evapotranspiration—Guidelines for Computing Crop Water Requirements—FAO Irrigation and Drainage Paper 56*, Rome, Italy: FAO, 1998, Art. no. D05109.
[105] G. J. M. De Lannoy, R. D. Koster, R. H. Reichle, S. P. P. Mahanama, and Q. Liu, "An updated treatment of soil texture and associated hydraulic properties in a global land modeling system," *J. Adv. Model. Earth Syst.*, vol. 6, no. 4, pp. 957–979, Dec. 2014.
[106] J. Šimůnek, M. Šejna, H. Saito, M. Sakai, and M. Th. van Genuchten, "The Hydrus-1D software package for simulating the movement of water, heat, and multiple solutes in variably saturated media, version 4.17," HYDRUS software series 3, Riverside, CA, USA: Dept. Environ. Sci., Univ. California Riverside, p. 342, 2013.
[107] A. Tabatabaeenejad, M. Burgin, X. Duan, and M. Moghaddam, "P-band radar retrieval of subsurface soil moisture profile as a second-order polynomial: First AirMOSS results," *IEEE Trans. Geosci. Remote Sens.*, vol. 53, no. 2, pp. 645–658, Feb. 2015.
[108] R. Fletcher, *Practical Methods of Optimization*. New York, NY, USA: Wiley, 1987, p. 4.
[109] A. V. M. Ines and B. P. Mohanty, "Near-surface soil moisture assimilation for quantifying effective soil hydraulic properties using genetic algorithm: 1. Conceptual modeling," *Water Resour. Res.*, vol. 44, no. 6, pp. 1–26, 2008.
[110] Y. Liu *et al.*, "Advancing data assimilation in operational hydrologic forecasting: Progresses, challenges, and emerging opportunities," *Hydrol. Earth Syst. Sci.*, vol. 16, no. 10, pp. 3863–3887, 2012.
[111] Y. Tramblay *et al.*, "Estimation of antecedent wetness conditions for flood modelling in northern Morocco," *Hydrol. Earth Syst. Sci.*, vol. 16, no. 11, pp. 4375–4386, 2012.
[112] E. Zehe, R. Becker, A. Bárdossy, and E. Plate, "Uncertainty of simulated catchment runoff response in the presence of threshold processes: Role of initial soil moisture and precipitation," *J. Hydrol.*, vol. 315, no. 1, pp. 183–202, 2005.
[113] R. H. Reichle, D. Entekhabi, D. B. Mclaughlin, and R. M. Parsons, "Downscaling of radio brightness measurements for soil moisture estimation: A four-dimensional variational data assimilation approach," *Water Resour. Res.*, vol. 37, no. 9, pp. 2353–2364, 2001.
[114] N. N. Das and B. P. Mohanty, "Root zone soil moisture assessment using remote sensing and vadose zone modeling," *Vadose Zone J.*, vol. 5, no. 1, pp. 296–307, 2006.

Parisa Heidary (Member, IEEE) received the B.Sc. and M.Sc. degrees in civil and environmental engineering from Sharif University of Technology, Tehran, Iran, in 2013 and 2016, respectively. She is currently working toward the Ph.D. degree with a focus on hydrology and water resource engineering with the Department of Civil and Environmental Engineering, George Washington University, Washington, DC, USA.

Her research interests include modeling soil water dynamics, land-atmosphere interactions, data assimilation, application of GIS, and remote sensing in hydrology.

Leila Farhadi (Member, IEEE) received the B.Sc. and M.Sc. degrees in civil and environmental engineering from the Sharif University of Technology, Tehran, Iran, and the Ph.D. degree in civil and environmental engineering with a focus on hydrology and water resources from the Massachusetts Institute of Technology, Cambridge, MA, USA, in 2001, 2003 and 2012, respectively.

Upon receiving the Ph.D. degree, in 2012, she worked as a Research Scientist with the Global Modeling and Assimilation Office of NASA, Goddard before joining the Department of Civil and Environmental Engineering, George Washington University (GWU), Washington, DC, USA, in 2013. She is currently an Associate Professor of Engineering with GWU. Her research interests include understanding and modeling land surface and land–atmosphere interaction and exchange processes by utilizing innovative remote sensing, optimization, and numerical modeling techniques.

Dr. Farhadi is the recipient of the National Science Foundation 2019 Early Career Faculty (CAREER) Award and the 2017 New (Early Career) Investigator award in Earth Sciences from the National Aeronautics and Space Administration.

Muhammad Umer Altaf (Member, IEEE) received the Ph.D. degree in applied earth science from the Delft University of Technology, Delft, The Netherlands, in 2011.

He is currently working as a Staff Scientist with the King Abdullah University of Science and Technology, Thuwal, Saudi Arabia. In the last few years, he has extensively been involved in the field of inverse modeling with focus on large-scale systems. His recent projects include developing common data assimilation tools for hydrological and related communities. His research interests include development and application of model order reduction methods within the optimization framework by avoiding complex adjoint model derivations.